OAK RIDGE NATIONAL LABORATORY
operated by
UNION CARBIDE CORPORATION
for the
U. S. ATOMIC ENERGY COMMISSION

ORNL - TM - 557

16

RESTRAINED THERMAL BOWING OF BEAMS ACCOMPANIED BY CREEP - WITH APPLICATION TO THE EXPERIMENTAL GAS-COOLED REACTOR FUEL ELEMENTS

J. M. Corum
W. A. Shaw

NOTICE

This document contains information of a preliminary nature and was prepared primarily for internal use at the Oak Ridge National Laboratory. It is subject to revision or correction and therefore does not represent a final report. The information is not to be abstracted, reprinted or otherwise given public dissemination without the approval of the ORNL patent branch, Legal and Information Control Department.

LEGAL NOTICE

This report was prepared as an account of Government sponsored work. Neither the United States, nor the Commission, nor any person acting on behalf of the Commission:

A. Makes any warranty or representation, expressed or implied, with respect to the accuracy, completeness, or usefulness of the information contained in this report, or that the use of any information, apparatus, method, or process disclosed in this report may not infringe privately owned rights; or

B. Assumes any liabilities with respect to the use of, or for damages resulting from the use of any information, apparatus, method, or process disclosed in this report.

As used in the above, "person acting on behalf of the Commission" includes any employee or contractor of the Commission, or employee of such contractor, to the extent that such employee or contractor of the Commission, or employee of such contractor prepares, disseminates, or provides access to, any information pursuant to his employment or contract with the Commission, or his employment with such contractor.

CONTENTS

	Page
ABSTRACT	4
INTRODUCTION	5
NOMENCLATURE	7
THEORETICAL CONSIDERATIONS	9
APPLICATION TO THE EXPERIMENTAL GAS-COOLED REACTOR FUEL ELEMENTS	21
CONCLUSIONS	25
APPENDIX A — RECTANGULAR AND SANDWICH-TYPE FUEL ELEMENTS	27
APPENDIX B — EFFECT OF UNEQUAL PROPERTIES DUE TO WIDELY VARYING TEMPERATURES	29
APPENDIX C — EXPERIMENTAL VERIFICATION	35
REFERENCES	37
FIGURES	38

JUN 10 1963

ABSTRACT

An analytical procedure is formulated for predicting the lateral deformation of a long slender beam when the material is subjected to creep conditions. The beam has simply-supported ends, is restrained at the midpoint, and is loaded by a temperature differential wherein the temperature is a linear function of the thickness. The creep strains are predicted by employing a constant-stress creep law consisting of a secondary or steady creep term only. Both the restraining force at the midpoint and the deflection profiles for the beam may be obtained as functions of time using the analytical method presented.

The analysis is applied to the Experimental Gas-Cooled Reactor fuel elements for several mean temperatures and temperature differentials, and, in every case, the limiting maximum deflection of a fuel rod is e/5.13, where e is the maximum deflection without a restraint at the midpoint. This is significant because, although an infinite time is required for a rod to reach its maximum deflection, this deflection will be closely approached during the projected fuel element residence time in the higher temperature regions of the reactor.

INTRODUCTION

Experimental and analytical studies have indicated that surface temperature variations will exist around the circumference of the rods in the fuel elements of the Experimental Gas-Cooled Reactor (EGCR) being built by the Atomic Energy Commission at Oak Ridge, Tennessee. These temperature variations will cause the long cylindrical fuel rods to bow. In order to limit the amount of deformation, spacers are attached to the rods at the midpoints.

It is the purpose of this report to describe the theoretical development and the application of an analytical model for predicting the high temperature behavior of a centrally restrained beam when the material is subjected to creep conditions. The analysis makes use of a constant-stress creep law consisting of a secondary or steady creep term only. An iteration procedure is used to obtain both the decay of the restraining force at the midpoint and the deflection profile of the beam as a function of time.

The procedure formulated is applied to the EGCR fuel rods to obtain the decay of the restraining forces at the midpoints and to obtain deflection curves for the elements with the passage of time. It is tacitly assumed that the deflection of each rod is dictated only by the cladding behavior. Mean temperatures of 1200, 1300, 1400, 1500, and 1600°F are considered with temperature differentials (linear with diameter) of 25, 50, and 100°F for each. The results are presented graphically.

The theoretical considerations are developed in a general manner so that the principles presented are applicable to a variety of different situations. The equations necessary to predict the high temperature behavior of both rectangular and sandwich-type fuel elements are given in Appendix A.

In the analysis presented, use is made of only one set of material constants, these being the constants corresponding to the mean temperature of the element. Actually, since the temperature varies across the

element, the temperature dependent material constants will also vary across the element. A discussion of the errors introduced through the use of constant material properties is given in Appendix B. The equations derived there may be used to predict both creep and elastic deflections of beams made of materials having unequal material properties in tension and in compression.

Experiments were performed on Plexiglas beams at room temperature to check the theoretical analysis. A description of the tests and the results obtained therefrom are given in Appendix C. Comparison of the experimental and theoretical results reveals that, at least qualitatively, the Plexiglas experiments verify the mathematical model.

NOMENCLATURE

a	Plate thickness of sandwich-type element
A	Cross-sectional area of a beam
b	Width of rectangular or sandwich-type element
B,n	Constants in creep law
d_i	Inside diameter of cylindrical fuel rod cladding
d_o	Outside diameter of cylindrical fuel rod cladding
D	Constant replacing EI in elastic beam equation when properties in tension and compression are not equal
e	Deflection, at $x = L/2$, of initial stress-free thermally bowed beam
E	Modulus of elasticity
h	Depth of a beam or element
I	Moment of inertia of beam cross section
I^*	Characteristic of beam geometry and the appropriate creep constants
K_1,K_2	Constants in temperature function
L	Length of a beam
m	Distance from neutral axis to the outer fibers of a cross section
M	Bending moment at any point along a beam
P	Concentrated force
R_i	Inside radius of cylindrical fuel rod cladding
R_o	Outside radius of cylindrical fuel rod cladding
T	Temperature
w	Total lateral deflection of a beam measured from the x axis
w'	Lateral deflection of a beam due to creep alone
w''	Lateral deflection of a beam due to elastic deformation alone
w_o	Initial deflection of a restrained beam measured from the x axis
x,y,z	Rectangular coordinates
y	Distance to a fiber measured from the neutral axis of a beam cross section
α	Linear coefficient of thermal expansion

β	Symbol denoting $P/2I^{*}B$
$\gamma_{xy}, \gamma_{yz}, \gamma_{zx}$	Shearing strain components in rectangular coordinates
ϵ_x, ϵ_y, ϵ_z	Unit elongations or strains in x, y, and z directions
ρ	Radius of curvature of a deflected beam
σ	Normal component of stress
τ	Time in hours
c	Subscript denoting compression
k	Subscript denoting terms of a series
t	Subscript denoting tension

THEORETICAL CONSIDERATIONS

In order to predict the behavior of a long slender fuel rod which is supported at the end points, restrained at the midpoint, and subjected to a temperature differential linear across the thickness, one must have expressions which describe the initial elastic behavior of the rod as well as the subsequent creep behavior. Thus, the problem becomes one of deriving the necessary equations and formulating a procedure for their use. In the following analysis the problem has been generalized to the case of an arbitrary beam subjected to the above conditions.

Unless all parts of a body are allowed to expand freely, a non-uniform temperature distribution in the body will cause thermal stresses. Consequently, in the case of a beam which is unrestrained, a temperature difference between opposite sides will deform the element. Stresses may or may not exist, depending on the manner in which the temperature is distributed across the unit. It may be shown that an unrestrained body subjected to a temperature distribution linear in rectangular space coordinates will not possess thermal stresses.[1] [1]

Consider a beam with the temperature linearly distributed across its thickness. The deformation, that is, bowing, of the beam will be the same regardless of whether the temperature is constant or linearly distributed along the length provided the difference across the element is the same. For zero stresses and a temperature distribution

$$T = K_1 x + K_2 y \quad , \tag{1}$$

Hooke's law gives

$$\begin{aligned} \epsilon_x = \epsilon_y = \epsilon_z &= \alpha K_1 x + \alpha K_2 y \\ \gamma_{xy} = \gamma_{yz} = \gamma_{zx} &= 0 \quad . \end{aligned} \tag{2}$$

---

[1] Numbers in brackets refer to references given at the end of this report.

The first term on the right hand side of the first of Eqs. (2) corresponds to a uniform extension of the beam with no rotation of the cross sections. The second term implies rotation of the cross sections such that plane sections remain plane as shown in Fig. 1. This rotation of the cross sections results in the bowing of the beam. When plane sections remain plane, the curvature of the center line of the beam is, from Fig. 2,

$$\frac{dx}{\rho} = \frac{\alpha K_2 y dx}{y}$$

or

$$\frac{1}{\rho} = \alpha K_2 \quad . \tag{3}$$

Since the curvature is constant with length, the configuration will be an arc of a circle. If the temperature differential existing between opposite sides of the beam is designated by ΔT, Eq. (1) yields

$$\Delta T = \left[K_1 x + K_2(h/2)\right] - \left[K_1 x - K_2(h/2)\right]$$

or

$$K_2 = \frac{\Delta T}{h} \quad , \tag{4}$$

where h is the total thickness of the beam. Substituting Eq. (4) in Eq. (3) gives

$$\frac{1}{\rho} = \frac{\alpha \Delta T}{h} \quad . \tag{5}$$

Using elementary beam theory, this becomes

$$\frac{d^2 w}{dx^2} = - \frac{\alpha \Delta T}{h} \quad . \tag{6}$$

Integrating and applying the boundary conditions

1) $w = 0$ at $x = 0$

2) $dw/dx = 0$ at $x = L/2$

yields

$$w = \frac{\alpha \Delta T}{2h} (Lx - x^2) \tag{7}$$

as the equation for the deflection of an unrestrained beam subjected to a temperature differential linear across the thickness.

Designating the maximum deflection, which occurs at $x = L/2$, as e, the following expression is obtained from Eq. (7).

$$e = \frac{\alpha \Delta T L^2}{8h} \tag{8}$$

Using this expression, Eq. (6) can be rewritten as

$$\frac{d^2w}{dx^2} = -\frac{8e}{L^2} \quad . \tag{9}$$

The preceeding equations completely define the behavior of an unrestrained beam subjected to a temperature difference linear across the diameter. However, in the problem under consideration the beam is not unrestrained but has a restraining force applied at the midpoint. Suppose that some mode of restraint is now applied at the midpoint of the initially unrestrained deformed beam so that zero deflection is obtained at that location. The elastic deflection as a function of length is again given by beam theory. Since the total deflection is the sum of the component from the temperature distribution, Eq. (7), and the component due to the external force system, the total curvature, d^2w/dx^2, is also a sum of the components. In this case,

$$\frac{d^2w}{dx^2} = \frac{M}{EI} - \frac{8e}{L^2} \quad , \tag{10}$$

where the second term is taken from Eq. (9). Referring to Fig. 3, the differential equation of the elastic curve with a concentrated load applied at the midpoint is

$$\frac{d^2w}{dx^2} = \frac{P}{2EI}\,x - \frac{8e}{L^2} \quad , \qquad x \leq L/2$$

$$\frac{d^2w}{dx^2} = \frac{P}{2EI}\,(L - x) - \frac{8e}{L^2} \quad , \quad x \geq L/2 \quad . \tag{11}$$

Since the system is symmetrical about the midpoint, only the first of Eqs. (11) need be considered. Integrating and applying the boundary conditions

1) $w = 0$ at $x = 0$
2) $dw/dx = 0$ at $x = L/2$

yields

$$w = \frac{Px}{48EI}\,(4x^2 - 3L^2) - \frac{4ex}{L^2}\,(x - L) \quad , \quad x \leq L/2 \quad . \tag{12}$$

The magnitude of the force, P_o, required to give zero deflection at the midpoint is, from Eq. (12),

$$P_o = \frac{48EI}{L^3}\,e \quad . \tag{13}$$

Equation (12), with P_o substituted for P, represents the initial thermal bowing of a beam restrained at the midpoint, provided the temperature difference is suddenly applied.

At sufficiently high temperatures the stresses in the restrained beam and consequently the force necessary to maintain zero deflection at the midpoint will be decreased due to creep of the material. The stress state of any arbitrary cross section is such that the creep deformation will bring about a change in the curvature of the beam. The

configuration and position of the center line of the beam after some period of time will depend upon the integrated effect over the entire length.

In the analysis of beams, Bernoulli's hypothesis that plane sections remain plane is assumed to hold at all times; its validity can be extended to pure bending under creep conditions.[2] The hypothesis when applied to a beam subject to creep implies that a transitional stress state is required for a shift from the linear distribution which occurs when the beam is first deflected (elastically) to some stable stress distribution where the creep rate for a given fiber is proportional to its distance from the neutral axis. Provided the temperature difference is suddenly applied, the stress and strain distribution at the instant of application are given by linear elastic theory. That is, sufficient time has not elapsed to allow the material to creep. This initial linear stress distribution will give a nonlinear creep strain distribution. This can be illustrated as follows: Consider a constant-stress creep law of the form

$$\dot{\epsilon} = \left(\frac{\sigma}{B}\right)^n \tag{14}$$

which consists of a secondary or steady-creep term only. Here, $\dot{\epsilon}$ denotes differentiation with respect to time, τ, and B and n are the so-called creep constants for a specified material at a given temperature. For a constant stress and a small time increment, $\Delta\tau$, Eq. (14) gives

$$\Delta\epsilon = \left(\frac{\sigma}{B}\right)^n \Delta\tau \quad . \tag{15}$$

From elastic beam theory, the initial stress distribution is

$$\sigma = \frac{My}{I} \quad ,$$

where y denotes the distance from the neutral axis to the fibers under consideration. Therefore, using Eq. (15),

$$\Delta\epsilon = \left(\frac{M}{BI}\right)^n y^n \Delta\tau \quad .$$

Since $\Delta\epsilon$ is nonlinear in y, plane sections will not remain plane due to creep alone. Instead, as creep progresses, the cross sections will deform to some curved line CD as shown in Fig. 4. This violates Bernoulli's hypothesis regarding plane sections remaining plane. The usual explanation is that the fibers also undergo elastic increments of strain during this transitional stage so that plane sections remain plane.[3] Thus, a fiber at a distance y from the neutral axis must have an elastic increment of stress to make the section plane. In analyzing a beam this additional increment of stress requires an elastic adjustment of the total stress state so that the internal resisting moment will remain equal to the applied moment.

Keeping the above considerations in mind and following the creep behavior with time, several effects may be observed. The load carried by the initially highly stressed fibers is decreased while the lower stressed inner fibers take up more of the load. After a certain time interval, the stresses reach a stable distribution and the creep rate of any fiber becomes only a function of the distance from the neutral axis. That is, the change in total strain, which has been hypothesized as linear in y, is due to creep alone. At this stable condition, the stress state is, in general, nonlinear as shown in Fig. 5.

The transitional stage, allowing all fibers to attain a minimum creep rate, may be neglected if the time required is short relative to the interval of the stable condition under scrutiny. This is usually done in the literature without so stating (see Ref. 4), and good agreement has been found between experimental data and solutions based on the stable creep stress supposition. Consequently, the transitional stage is neglected in deriving the equation describing the creep deflection of a beam.

The above description of the creep phenomenon utilizes a constant-stress creep law to determine strains occurring during transitional or variable stress states because, as yet, no satisfactory creep law has been formulated for variable stress conditions. However, the convergence to the stable state can be arrived at by considering time increments sufficiently small so that the variation of stress over each time interval is negligible relative to the total value.

The creep law previously chosen has been shown to give good agreement with experimental results from tests on type 304 stainless steel. Considering a small time interval $\Delta\tau$, Eq. (15) gives the change in strain due to a given stress acting over the time interval. Referring to Fig. 6, and assuming the creep properties to be equal in tension and in compression, Bernoulli's hypothesis that plane sections remain plane yields

$$\frac{dx}{\rho} = \frac{\Delta\epsilon}{y}\, dx$$

or

$$\Delta\epsilon = y/\rho \quad . \tag{16}$$

Substituting Eq. (16) into Eq. (15) and solving for σ yields

$$\sigma = B\left(\frac{y}{\rho\Delta\tau}\right)^{1/n} \quad . \tag{17}$$

Two conditions of equilibrium are available. Since it is assumed that the material properties are the same in tension and compression, the first equilibrium condition states that the neutral axis passes through the centroid of each cross section. The second condition states that the applied moment must equal the resisting moment; therefore,

$$M = \int_A \sigma y dA$$

or using Eq. (17),

$$M = \int_A B\left(\frac{1}{\rho\Delta\tau}\right)^{1/n} \left|y\right|^{\frac{n+1}{n}} dA \quad . \tag{18}$$

Integrating,

$$M = BI^*\left(\frac{1}{\rho\Delta\tau}\right)^{1/n} \tag{19}$$

where

$$I^* = \int_A \left|y\right|^{\frac{n+1}{n}} dA \quad . \tag{20}$$

Substituting Eq. (17) into Eq. (19), the following expression is obtained for the stress distribution across a beam during creep.

$$\sigma = \frac{My^{1/n}}{I^*} \tag{21}$$

Note the similarity between Eq. (21) and the corresponding equation,

$$\sigma = \frac{My}{I} \quad ,$$

for the elastic case.

Using Eq. (21) in Eq. (15) yields

$$\Delta\epsilon = \left(\frac{M}{I^*B}\right)^n y\,\Delta\tau \quad . \tag{22}$$

Substituting Eq. (22) into Eq. (16) gives

$$1/\rho = \left(\frac{M}{I^*B}\right)^n \Delta\tau \approx \frac{d^2w'}{dx^2} \quad . \tag{23}$$

This is the creep equation defining the change in curvature, which occurs during the time interval $\Delta\tau$, due to a moment $M(x)$ which is constant over the time interval. This equation for the creep case corresponds to

$$1/\rho = \frac{M}{EI}$$

for the elastic case.

In the particular case under consideration, where zero deflection at the midpoint is maintained by a concentrated force, P,

$$M = \frac{P}{2} x \quad , \qquad x \leq L/2 \quad .$$

Therefore, Eq. (23) becomes

$$\frac{d^2 w'}{dx^2} = \beta^n \Delta\tau \, x^n \quad , \tag{24}$$

where

$$\beta = \frac{P}{2I^* B} \quad . \tag{25}$$

Performing two successive quadratures on Eq. (24) subject to the boundary conditions

1) $w' = 0$ at $x = 0$

2) $\frac{dw'}{dx} = 0$ at $x = L/2$,

the following equation is obtained for the creep deflection which occurs at any point ($0 \leq x \leq L/2$) during the time interval $\Delta\tau$.

$$w' = \frac{\beta^n \Delta\tau}{n+1} \left[\frac{x^{n+2}}{n+2} - (L/2)^{n+1} x \right] \tag{26}$$

Remembering that in the actual problem the moment distribution continually changes with time, an approximate solution to the time dependent behavior of the beam is obtained in the following manner. The moment distribution and, therefore, the stresses and creep rates are assumed to remain constant for a small time interval. These conditions will give a new configuration which may, or may not, violate geometrical restrictions. If a violation exists, the geometry is "adjusted" using elastic theory. A new moment distribution differing from the original function is then obtained according to the dictates of the new loading. Repeating this procedure by taking additional small time intervals, the complete behavior of the beam, as a function of time, may be predicted. This same reasoning, regarding adjustment of the geometry of the structure to a required configuration by elastic theory, has been used in discussing relief of thermal stresses in infinitely long cylinders by creep.[5]

The adjustment and iteration procedure for the problem considered herein consists of the following detailed steps: Calculate the initial force P_o necessary to maintain zero deflection at the midpoint of the beam by Eq. (13). Choose a small time interval, $\Delta\tau_1$, and by the use of Eq. (26) and the appropriate creep constants, calculate the creep deflection w' due to force P_o acting for time $\Delta\tau_1$. When this deflection is added to the initial elastic deflection, a new configuration for the center line of the element is obtained which violates the geometrical condition of zero deflection at the midpoint. Therefore, the beam is restored to its initial position at the midpoint by elastic beam theory. This is done by calculating the increment of force ΔP_1 necessary to elastically restore the beam to its original position at the midpoint. This increment of force which is of opposite sign to P_o is then used in the elastic deflection equation for the beam, and the deflection obtained therefrom is added to the deflection which violated the geometry. The beam deflection at the midpoint is now zero, but the deflection at other points is not necessarily equal to the initial deflection at those points. At this time, the force P_o is no longer acting on the beam; instead, a

new force P_1 which is equal to P_o plus ΔP_1 is acting at the midpoint. A new small time increment, $\Delta\tau_2$, is arbitrarily chosen, and the entire procedure is repeated.

The procedure can best be visualized by referring to Fig. 7 which depicts the assumed behavior of a beam during an arbitrary time interval, $\Delta\tau_i$. Since the deflection at any point other than the midpoint will not necessarily return to its original value when the midpoint is brought back to zero, the curvature and deflection of the beam will change due to creep of the material. Referring to Fig. 7 again, the position w_i of the element after time

$$\tau = \sum_{k=o}^{i} \Delta\tau_k \tag{27}$$

is given by

$$w_i = w_{i-1} + w_i' + w_i'' \quad , \tag{28}$$

where w_{i-1} is the total deflection at time $\tau - \Delta\tau_i$, w_i' is the creep deflection due to force P_{i-1} acting for a time interval $\Delta\tau_i$, and w_i'' is the elastic deflection due to the increment of force ΔP_i, which is a negative quantity. The initial deflection w_o is given, in terms of e, by Eq. (12) with Eq. (13) defining P. Therefore,

$$w_o = \frac{4e}{L^3} x^3 - \frac{4e}{L^2} x^2 + \frac{e}{L} x \quad , \qquad x \leq L/2 \quad . \tag{29}$$

Using the values P_{i-1} and $\Delta\tau_i$ in Eqs. (25) and (26), an expression for w_i' is obtained. Finally, w_i'' is given by elementary beam theory as

$$w_i'' = \frac{\Delta P_i}{48EI} (4x^3 - 3L^2x) \quad , \qquad x \leq L/2 \quad . \tag{30}$$

Setting the derivative of Eq. (29) equal to zero, it is seen that the initially restrained beam has a maximum deflection of 2e/27 at x equal L/6; however, it should not be assumed that after some arbitrary time the maximum deflection will remain at this location.

Equations (25) through (30) can be applied to any case where a beam subjected to a temperature differential, linear with thickness, is simply-supported at the ends and fixed at the midpoint. The problem of computing the deflections as a function of x and time is rather involved. However, the task is greatly simplifed by choosing several locations along the beam and calculating the time dependent deflections at these points. In this manner a family of curves may be plotted showing the position of a beam at the end of each time interval.

APPLICATION TO THE EXPERIMENTAL GAS-COOLED REACTOR FUEL ELEMENTS

The Experimental Gas-Cooled Reactor (EGCR) is a combined experimental and power demonstration reactor which is being built by the Atomic Energy Commission at Oak Ridge, Tennessee. It is fueled with enriched uranium dioxide pellets clad in type 304 stainless steel tubes. A fuel assembly consists of a cluster of seven cylindrical stainless steel tubes (containing the enriched UO_2 pellets) spaced and supported within a cylindrical graphite sleeve. A stack of six assemblies plus one dummy each at the top and bottom fill a fuel channel in the graphite core of the reactor. A drawing of the EGCR fuel assembly is shown in Fig. 8.

Each fuel rod is 27.5 in. long. The stainless steel cladding has an outside diameter of 0.75 in. with a wall thickness of 0.020 in. The rods are supported within the graphite sleeve by stainless steel spiders at the top and bottom. In order to limit the lateral movement of the rods, spacers are attached to each rod at the midpoint as shown in Fig. 8.

Experimental and analytical studies have indicated that surface temperature variations will exist around the circumference of the fuel rods. These differences result primarily from variations in the local heat transfer coefficients caused by unsymmetrical flow of the helium coolant through the assembly and from nonsymmetrical heat generation within each unit. Taking the temperature gradient to be linear across a rod, the end restraints to be simple supports, and assuming that the rod deflection is dictated only by the cladding behavior, the problem of predicting the creep behavior with time reduces to that of the simply-supported beam restrained at the midpoint as previously discussed.

The properties of the cladding material (type 304 stainless steel) are given in Table 1 for the temperatures shown. Using Eqs. (25) through (30), the iteration procedure was programmed for calculation on the

Table 1. Properties of Type 304 Stainless Steel

Mean Temperature (°F)	α^a(1/°F)	E(psi)	n^b	$B^b\left[(hr)^{1/n}\ lb/in.^2\right]$
1200	11.78×10^{-6}	21.0×10^6	6.0	73.2×10^3
1300	11.98×10^{-6}	20.0×10^6	6.0	44.4×10^3
1400	12.18×10^{-6}	19.0×10^6	6.0	29.3×10^3
1500	12.38×10^{-6}	18.0×10^6	6.0	21.3×10^3
1600	12.58×10^{-6}	17.0×10^6	5.8	15.0×10^3

[a]Local (at temperature) coefficient of thermal expansion.
[b]From relaxation tests performed by ORNL Metallurgy Division.

IBM-704 digital computer. For the symmetrical cladding cross section, Eq. (20) may be written

$$I^* = 2 \int_{A_T} y^{\frac{n+1}{n}}\, dA$$

where A_T denotes the area of the top half of the cross section. This expression becomes

$$I^* = 4 \int_0^{R_o} y^{\frac{n+1}{n}} \left(R_o^2 - y^2\right)^{1/2} dy - 4 \int_0^{R_i} y^{\frac{n+1}{n}} \left(R_i^2 - y^2\right)^{1/2} dy \quad .$$

After expanding the square root terms by the binominal theorem, simplifying, and integrating, the following expression is obtained.

$$I^* = -4nQ \left[-\frac{1}{1+2n} + \sum_{k=1}^{\infty} a_k \frac{1}{1+2(k+1)n} \right]$$

where

$$a_k = \frac{2k-3}{2k} \cdot a_{k-1} \quad , \quad k > 0 \quad ; \quad a_o = -1 \quad ,$$

and

$$Q = (0.375)^{\frac{3n+1}{n}} - (0.355)^{\frac{3n+1}{n}} \quad .$$

Using this expression for I^*, calculations were made to obtain the decay of the restraining forces at the midpoints and to obtain deflection profiles for the rods as a function of time.

Figures 9 through 13 are plots of the restraining force necessary to maintain zero deflection at the midpoint of a rod as a function of time. Mean temperatures of 1200, 1300, 1400, 1500, and 1600°F were considered, with temperature differentials of 25, 50, and 100°F for each.

Figures 14 through 28 are plots depicting the position of a rod with time as a parameter. Mean temperatures of 1200, 1300, 1400, 1500, and 1600°F were again considered with temperature differentials of 25, 50, and 100°F for each. Only one half of the length of the rod is represented because of symmetry. The curves labeled "initial elastic curve at 0 time" show the position of the rod immediately after the temperature gradient is applied but before any creep has taken place. The remaining curves are the positions of the rod after the designated time periods have elapsed. The curves labeled "∞ time" are the limiting positions the rods may be expected to reach. When these profiles are reached, the stresses are completely decayed. The initial elastic curve has a maximum deflection of e/13.5 which occurs at x = 4.58 in. However, as time passes, the maximum deflection moves toward the quarter position of the rod.

The spacing between each rod in the cluster is initially 0.250 in., and the spacing between the outer rods and the graphite support sleeve is initially 0.125 in. Observing the maximum deflections reached in

Figs. 14 through 28, it is seen that these deflections are small compared to the clearances between adjoining rods and between the graphite sleeve and the outer rods.

In order to compare the deflection rates for the curves plotted in Figs. 14 through 28, the maximum deflection at time, τ, was divided by the maximum deflection at τ equal infinity to obtain a dimensionless parameter. Figure 29 shows the results of these calculations; here, $w_{max}/w_{max_{\tau=\infty}}$ is plotted as a function of time for each of the cases shown in Figs. 14 through 28. As τ approaches infinity, the curves approach a value of one by definition, and at τ equal zero the curves converge toward a common value of ~0.38. Thus, the limiting deflection appears, in every case, to be a constant multiple of the maximum, initial deflection. Since the maximum, initial deflection is e/13.5, it may be concluded that any restrained rod will have a limiting maximum deflection of e/5.13. This is very significant because from Fig. 29 it may be seen that, although an infinite time is required for a rod to reach its maximum deflection, this deflection is closely approached during the projected residence time of the elements in the higher temperature regions of the reactor.

The maximum bowing deflection for an unrestrained tube whose length is one half that of the EGCR cladding is e/4. Hence, the limiting deflection under creep conditions approaches that which would occur if the center of the rod acted as a plastic hinge.

CONCLUSIONS

The theoretical analysis was formulated in terms of an arbitrary beam simply supported at the end points, restrained at the midpoint, and subjected to a temperature differential linear across the thickness. The creep equations were derived for a generalized loading so that the analysis presented may be extended, either in part or in whole, to a variety of problems involving creep of beams under various conditions.

Regarding the application to the EGCR fuel elements, the most significant result is that in every case the limiting maximum deflection which a fuel rod may be expected to reach is given by

$$y_{max} = e/5.13 \quad .$$

Here, e is the maximum deflection of an unrestrained rod subjected to the same temperature differential and is given by

$$e = \frac{\alpha \Delta T L^2}{8 d_o} \quad .$$

It is significant to note that the limiting deflection under creep conditions approaches that which would occur if the midpoint of the rod acted as a plastic hinge. In that case, the maximum deflection is given by e/4. Although an infinite amount of time is required for a rod to reach its maximum deflection, this deflection is closely approached during the projected residence time of the elements in the higher temperature regions of the reactor. Thus, for any given temperature differential, the maximum deflection of the rod may be immediately predicted.

APPENDIX A

RECTANGULAR AND SANDWICH-TYPE FUEL ELEMENTS

The bowing and creep behavior of several types of fuel elements may be examined using the procedure and equations presented. As two examples, other than the cylindrical EGCR fuel rods, solid rectangular elements and sandwich-type elements will briefly be considered.

In the case of a solid element with a rectangular cross section of height h and width b, I^* becomes

$$I^* = \frac{2bn}{2n+1} (h/2)^{\frac{2n+1}{n}} \quad . \tag{A1}$$

The following differential equation defining the creep deflection occurring during time $\Delta\tau$ is obtained by combining Eqs. (A1) and (23).

$$\frac{d^2w'}{dx^2} = \left[\frac{(2n+1)\ M}{2bnE}\right]^n (2/h)^{2n+1} \Delta\tau \tag{A2}$$

In this equation the symbol M denotes the moment distribution for any transverse loading. If the element is restrained at the midpoint by a force P, the moment will be

$$M = \frac{Px}{2} \quad , \quad x \leq L/2 \quad . \tag{A3}$$

Considering a sandwich-type element and referring to Fig. A1, the following expression is obtained for I^*.

$$I^* = \frac{2bn}{2n+1} \left[(h/2)^{\frac{2n+1}{n}} - (h/2 - a)^{\frac{2n+1}{n}}\right] \tag{A4}$$

Substituting Eq. (A4) into Eq. (23), the following differential equation defining the creep deflection occurring during time $\Delta\tau$ is obtained.

$$\frac{d^2w'}{dx^2} = \left\{ \frac{(2n+1)\ M}{2bBn\left[(h/2)^{\frac{2n+1}{n}} - (h/2 - a)^{\frac{2n+1}{n}}\right]} \right\}^n \Delta\tau \qquad \text{(A5)}$$

The symbol M denotes the moment distribution for any transverse loading.

APPENDIX B

EFFECT OF UNEQUAL PROPERTIES DUE TO WIDELY VARYING TEMPERATURES

By referring to Table 1 on page 22, which gives the properties of type 304 stainless steel, it is seen that both the elastic properties and the creep properties are significantly temperature dependent. The theoretical analysis previously described made use of only one set of material constants, these being the constants corresponding to the mean temperature. Actually, the temperature and, consequently, the material properties vary across the element. Thus, it is desirable to predict the error introduced by using mean temperature properties, especially when large temperature differentials exist. By comparing the curvature expressions for both creep and elastic deformation when unequal properties are employed to those for constant properties, a measure of the error may be obtained. In view of this end, it is necessary to derive the equations defining the curvatures for both elastic and creep deflections when the properties are not assumed constant.

The previous analysis may be extended to the case where a material has unequal properties in tension and in compression by following a method similar to that set forth in Reference [6]. Using this type of analysis, an approximation to the problem of widely varying temperatures may be obtained by assuming that all fibers in tension are at one mean temperature and that all fibers in compression are at a different mean temperature. For example, if the temperature on one side of a fuel element is 1550°F, the temperature in the middle is 1450°F, and the temperature on the opposite side is 1350°F, one could use the properties at 1500°F for the material in compression and those at 1400°F for the material in tension.

Keeping this observation in mind, the necessary equations will be derived using properties with the subscript t denoting tension and the

subscript c denoting compression. In this discussion, the equations describing the change in curvature due to creep will be derived first. The assumption that plane sections remain plane will again be made. The effect of unequal creep properties displaces the neutral axis to a position not passing through the centroid of the cross section. Thus, the problem becomes one of finding not only the curvature, $1/\rho$, but also the position of the neutral axis as a function of the resisting moment and the time interval $\Delta\tau$. Equation (15) may be written separately for the material in tension and for the material in compression as follows.

$$\Delta\epsilon_t = \left(\frac{\sigma_t}{B_t}\right)^{n_t} \Delta\tau \ , \quad \Delta\epsilon_c = \left(\frac{\sigma_c}{B_c}\right)^{n_c} \Delta\tau \tag{B1}$$

Referring to Fig. B1, the following relationships similar to those of Eq. (16) may be written.

$$\Delta\epsilon_t = \frac{y_t}{\rho} \quad , \quad \Delta\epsilon_c = \frac{y_c}{\rho} \ . \tag{B2}$$

Combining Eqs. (B1) and (B2) and solving for σ_t and σ_c, one obtains

$$\sigma_t = B_t \left(\frac{y_t}{\rho\Delta\tau}\right)^{1/n_t} \quad \text{and} \quad \sigma_c = B_c \left(\frac{y_c}{\rho\Delta\tau}\right)^{1/n_c} \ . \tag{B3}$$

To have equilibrium, the applied moment must equal the resisting moment; therefore,

$$M = \int_{A_t} B_t \left(\frac{1}{\rho\Delta\tau}\right)^{1/n_t} (y)^{\frac{n_t+1}{n_t}} dA + \int_{A_c} B_c \left(\frac{1}{\rho\Delta\tau}\right)^{1/n_c} (y)^{\frac{n_c+1}{n_c}} dA \ . \tag{B4}$$

Integrating, this becomes

$$M = B_t I_t^* \left(\frac{1}{\rho\Delta\tau}\right)^{1/n_t} + B_c I_c^* \left(\frac{1}{\rho\Delta\tau}\right)^{1/n_c} \tag{B5}$$

where

$$I_t^* = \int_{A_t} (y_t)^{\frac{n_t+1}{n_t}} dA \quad , \qquad I_c^* = \int_{A_c} (y_c)^{\frac{n_c+1}{n_c}} dA \quad . \tag{B6}$$

The neutral axis is defined by the condition of equilibrium stating that the resultant stress on the cross section is zero, or

$$\int_{A_t} \sigma_t \, dA + \int_{A_c} \sigma_c \, dA = 0 \quad . \tag{B7}$$

Substituting Eqs. (B3) into Eq. (B7) and integrating, the following relation is obtained.

$$B_t Z_t^* \left(\frac{1}{\rho \Delta\tau}\right)^{1/n_t} = B_c Z_c^* \left(\frac{1}{\rho \Delta\tau}\right)^{1/n_c} \tag{B8}$$

In this equation,

$$Z_t^* = \int_{A_t} (y_t)^{1/n_t} dA \qquad \text{and} \qquad Z_c^* = \int_{A_c} (y_c)^{1/n_c} dA \quad . \tag{B9}$$

Equations (B5) and (B8) may be solved simultaneously to obtain expressions for m_t or m_c and the curvature, $1/\rho$, in terms of the resisting moment, M, and the time increment, $\Delta\tau$. The symbol m refers to the distances from the neutral axis to the extreme fibers. By the above procedure one obtains expressions of the form

$$1/\rho = f\left[M(x), \Delta\tau\right] \tag{B10}$$

and

$$m_t = g\left[M(x), \Delta\tau\right] \quad . \tag{B11}$$

Equation (B10) represents the expression describing the change in curvature, due to creep, which occurs during the time interval $\Delta\tau$.

The elastic relationships may be obtained in a manner similar to the one followed for the creep equations. From statics, the applied moment must equal the resisting moment or,

$$\int_{A_t} y_t \, \sigma_t \, dA + \int_{A_c} y_c \, \sigma_c \, dA = M \quad . \tag{B12}$$

Using Hooke's law along with the geometry of the deformed beam, this expression may be written as follows.

$$M = \frac{E_t}{\rho} \int_{A_t} y_t^{\,2} \, dA + \frac{E_c}{\rho} \int_{A_c} y_c^{\,2} \, dA \tag{B13}$$

The stress resultant for any cross section is zero; hence,

$$E_t \int_{A_t} y_t \, dA + E_c \int_{A_c} y_c \, dA = 0 \quad . \tag{B14}$$

Equations (B13) and (B14), describing the elastic behavior, correspond to Eqs. (B5) and (B8) for the creep behavior. For elastic deflections where no creep has taken place, Eq. (B14) yields a value of m_t which is a constant. This value may be substituted into Eq. (B13) to give an expression of the form

$$1/\rho = M/D \quad . \tag{B15}$$

The constant D replaces EI in the conventional formula.

The problem of predicting the error introduced by using constant elastic and creep properties is made difficult by the fact that the variables involved are not separable. These variables influence the

behavior of the element in such a way that the deflection can be either more or less than for the case of constant properties depending on the relative increase or decrease in the property values across the element. Thus, for the particular case of type 304 stainless steel, the effect is best demonstrated by taking a specific example.

Using the cross section and temperature distribution shown in Fig. B2, the fibers in tension may be assumed to be at a mean temperature of 1300°F, while those in compression are at a mean temperature of 1500°F. The mean temperature of the element is 1400°F. Using the material properties as given in Table 1 on page 22, Eq. (B14), for the elastic case, yields $m_t = 0.97$ and $m_c = 1.03$. Substituting these values into Eq. (B13) gives

$$1/\rho = \frac{M}{12.64 \times 10^6} \quad .$$

Using the conventional formula and the value of E at 1400°F, one obtains

$$1/\rho = \frac{M}{12.67 \times 10^6} \quad .$$

The error introduced into the constant by using the value of E at the mean temperature of the beam is only 0.19%. This error is well within the range of accuracy which one would expect in reported values of E. Equations (B5) and (B8), describing the creep behavior, yield $m_t = 0.70$ and $m_c = 1.30$. Then, the curvature is given by

$$1/\rho = \frac{M^6 \Delta\tau}{373 \times 10^{24}} \quad .$$

Using Eq. (23) and the creep properties at 1400°F, one obtains

$$1/\rho = \frac{M^6 \Delta\tau}{390 \times 10^{24}} \quad .$$

The error introduced into the constant by using the creep constants corresponding to the mean temperature of the beam is 4.55%. This error is again within the range of accuracy which one would expect in the material constants.

In addition to the elastic and creep constants, the coefficient of thermal expansion, α, also varies across the element. Assume that there exists a large linear temperature differential across the element. Since α is approximately a linear function of temperature, the extension of fibers across the element is a quadratic function of the position, and thus, thermal stresses will be set up. However, referring to the values of α in Table 1, the variation over the temperature range shown in Fig. B2 is small. Taking the value of 1200°F as the mean value, the maximum variation from this mean is 3.29%. Thus, the extension of fibers across the beam will vary only slightly from a linear distribution.

The deformation of the beam is directly proportional to the curvature. Therefore, from the above observations, one may conclude that in calculating the behavior of an element made of type 304 stainless steel the error introduced by using constant material properties, corresponding to the mean temperature of the element, is small even for the large temperature differential considered.

APPENDIX C

EXPERIMENTAL VERIFICATION

During the course of the theoretical work, it became desirable to verify, experimentally, the behavior of a fuel rod as predicted by the mathematical model. The creep properties of Plexiglas (and Lucite) have been investigated at room temperature[6], and good agreement has been established between experimental and theoretical results making use of creep properties as determined for a creep law of the general form given by Eq. (14). There are two basic differences between the creep behavior of Plexiglas at room temperature and type 304 stainless steel at elevated temperatures. First, Plexiglas exhibits a noticeable primary stage of creep while type 304 stainless steel does not, and, second, the creep properties of Plexiglas are different in tension and in compression. The high primary creep rate of Plexiglas enables one to obtain, in a few hours at room temperature, results which are qualitatively commensurate to the behavior of a fuel element at an elevated temperature.

As long as a rod remains essentially straight the time dependent behavior does not depend on the initial stress-free configuration, that is, the equations describing the elastic and creep behavior are based only on changes in curvature. Thus, as long as the assumption from elementary beam theory that the length of the arc of the deflected curve is approximately equal to its chord length is not violated, the conditions for the rod may be duplicated simply by applying a concentrated load at the midpoint of a straight beam so that a constant center deflection is maintained. If this force is applied to the upper side of the beam, the fibers on that side are in compression while those on the opposite side are in tension. Hence, any ensuing creep deformation will allow the elements between the ends and the midpoint of the beam to move towards their initial stress-free positions along a path perpendicular to the

neutral axis, as shown in Fig. C1.

Several Plexiglas beams 22 in. long, 1/2 in. high, and 1 in. wide were tested. The testing fixture was devised to allow for variation in the maximum deflection from test to test, and a means was provided to mount dial gages at various points along the length of the beam. The testing fixture is shown in Fig. C2. The dial gage readings were corrected to obtain the actual movement of the beam perpendicular to the neutral axis.

Assuming that the initial elastic curve was a straight line, Fig. C3 represents the experimentally obtained growth curves for a maximum initial deflection, e, of 3 in. Figure C4 shows the displacement curves for the cylindrical EGCR rod at 1600°F with a temperature difference across the rod of 50°F. These curves are also shown with an initial straight line elastic curve in order that they might be compared directly with those in Fig. C3. A comparison of the theoretically and experimentally obtained curves reveals that, at least qualitatively, the Plexiglas experiment verifies the mathematical model.

REFERENCES

(1) A. S. Thompson and O. E. Rodgers, Thermal Power From Nuclear Reactors, John Wiley and Sons, New York, 1956, p 183.

(2) G. H. MacCullough, "An Experimental and Analytical Investigation of Creep in Bending," Trans. ASME 55, APM 55(1933).

(3) E. P. Popov, "Bending of Beams With Creep," J. Appl. Phys. 20, 251(1949).

(4) J. Marin, "Determination of the Creep Deflection of a Rivet in Double Shear," Trans. ASME, J. Appl. Mechanics Series E 81(3) 285(1959).

(5) H. Poritsky and F. A. Fend, "Relief of Thermal Stresses Through Creep," J. Appl. Mechanics 25, 589(1958).

(6) J. Marin, Y. Pao, and G. Cuff, "Creep Properties of Lucite and Plexiglas for Tension, Compression, Bending, and Torsion," Trans. ASME 73, 705(1951).

Other Related References

(1) I. Finnie, "Steady Creep of a Tube Under Combined Bending and Internal Pressure," ASME Paper No. 59-Met-5.

(2) Y. Pao and J. Marin, "Deflection and Stresses in Beams Subjected to Bending and Creep," J. Appl. Mechanics 19, 478(1952).

UNCLASSIFIED
ORNL-LR-DWG 50541

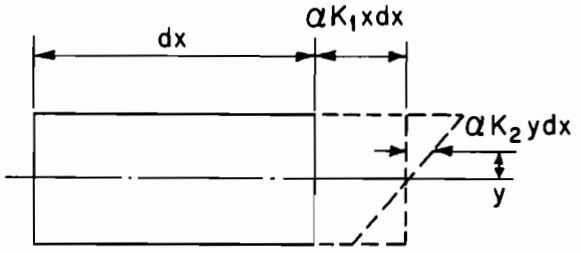

FIG. 1

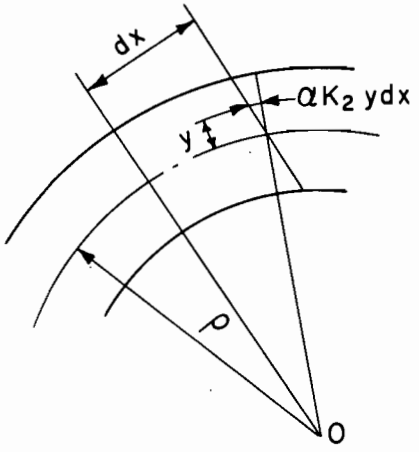

FIG. 2

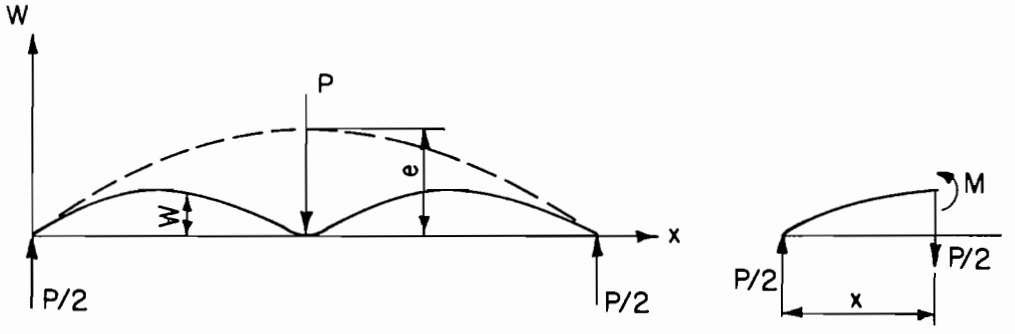

FIG. 3

UNCLASSIFIED
ORNL-LR-DWG 50542

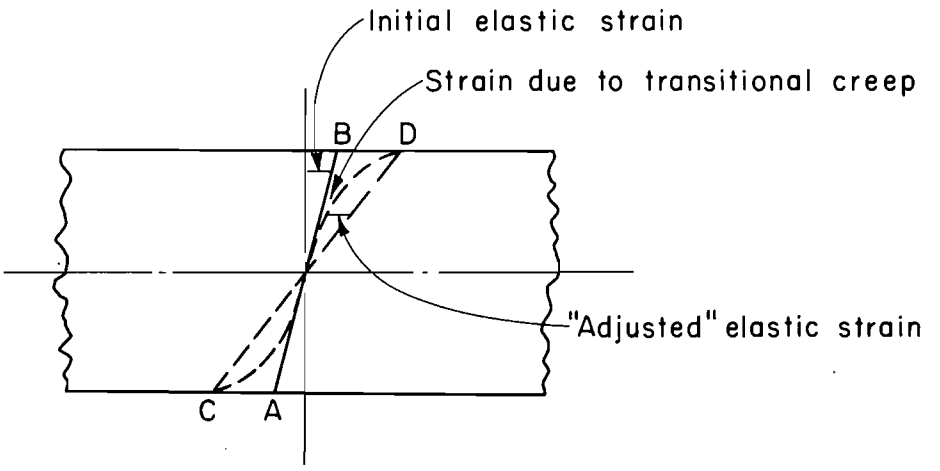

FIG. 4

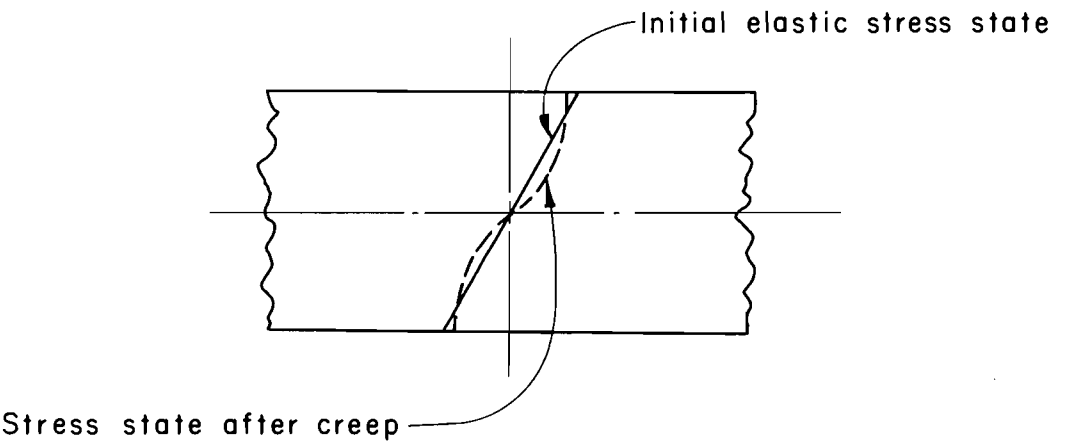

FIG. 5

UNCLASSIFIED
ORNL-LR-DWG 50543

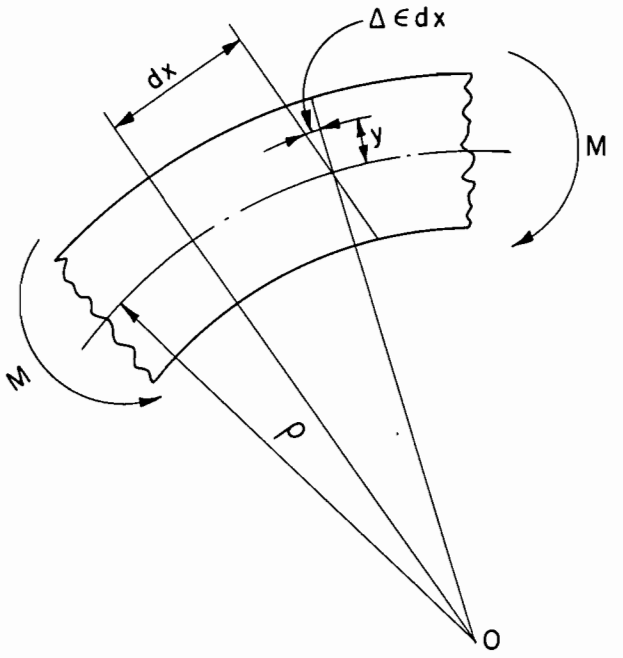

FIG. 6

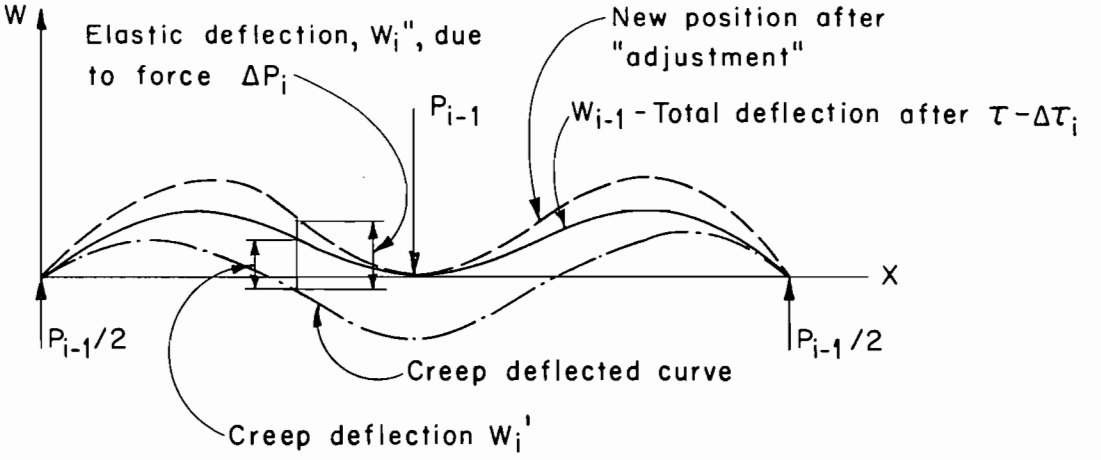

FIG. 7

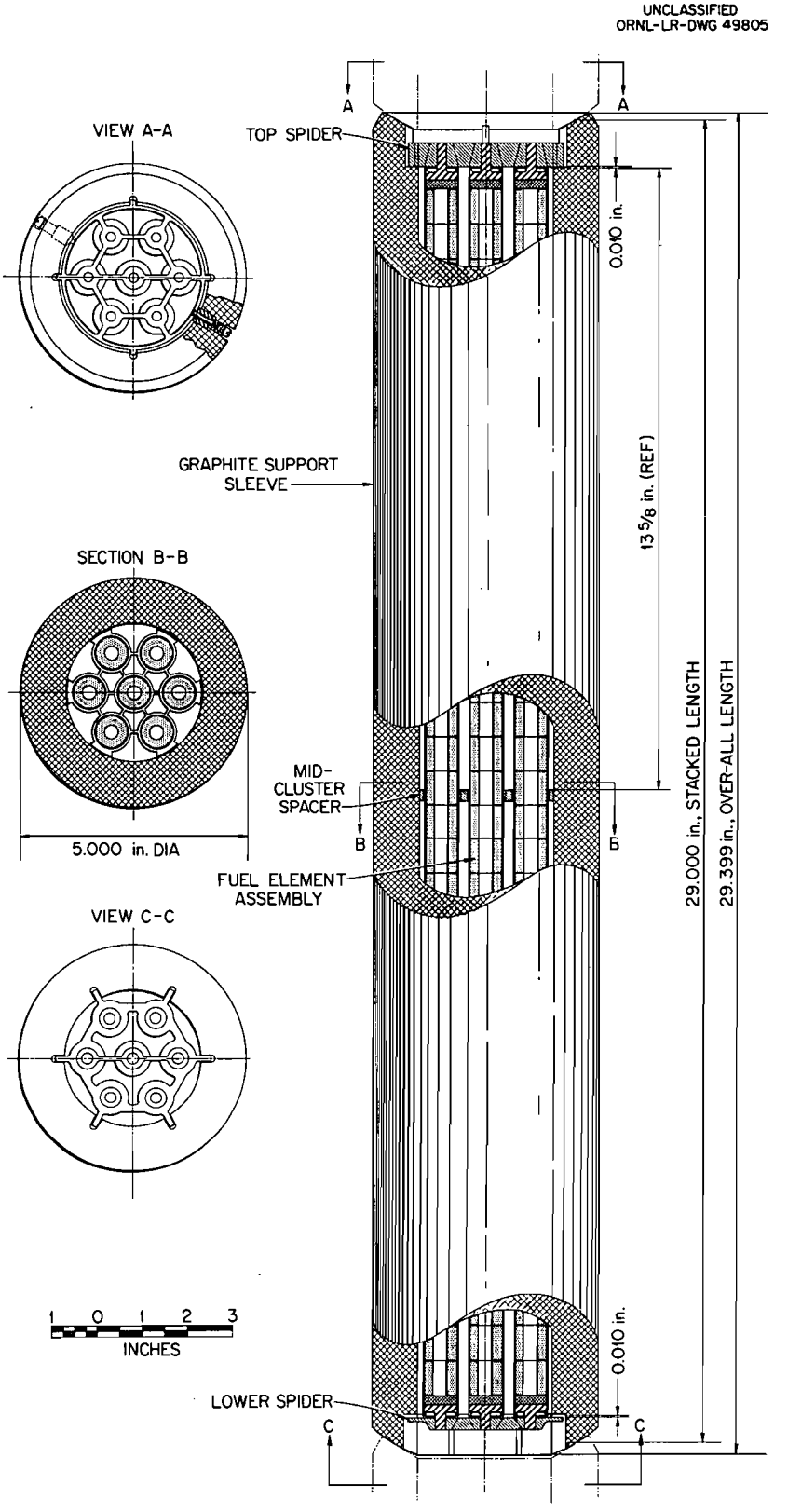

Fig. 8. Fuel Assembly for the Experimental Gas-Cooled Reactor.

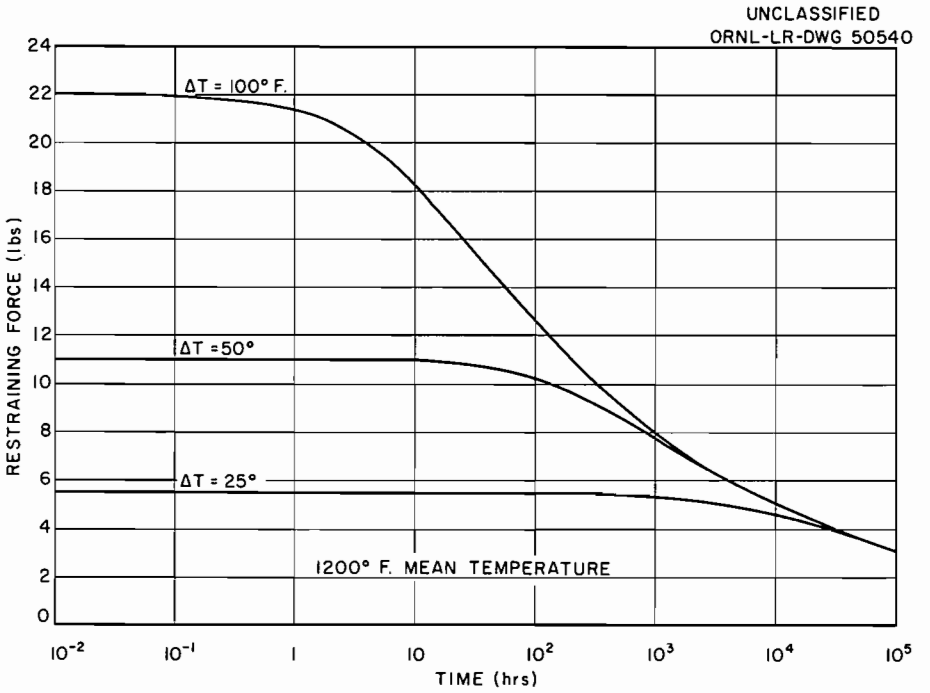

Fig. 9. Force Necessary to Restrain Midpoint of EGCR Fuel Rod as a Function of Time for a Mean Temperature of 1200°F and Diametrical Temperature Differences of 25, 50, and 100°F.

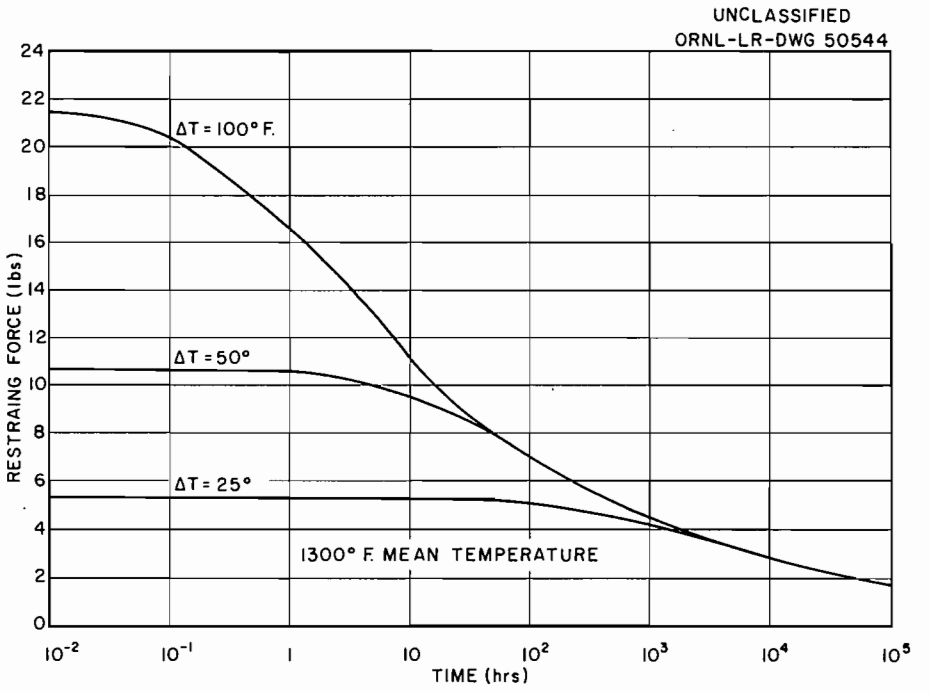

Fig. 10. Force Necessary to Restrain Midpoint of EGCR Fuel Rod as a Function of Time for a Mean Temperature of 1300°F and Diametrical Temperature Differences of 25, 50, and 100°F.

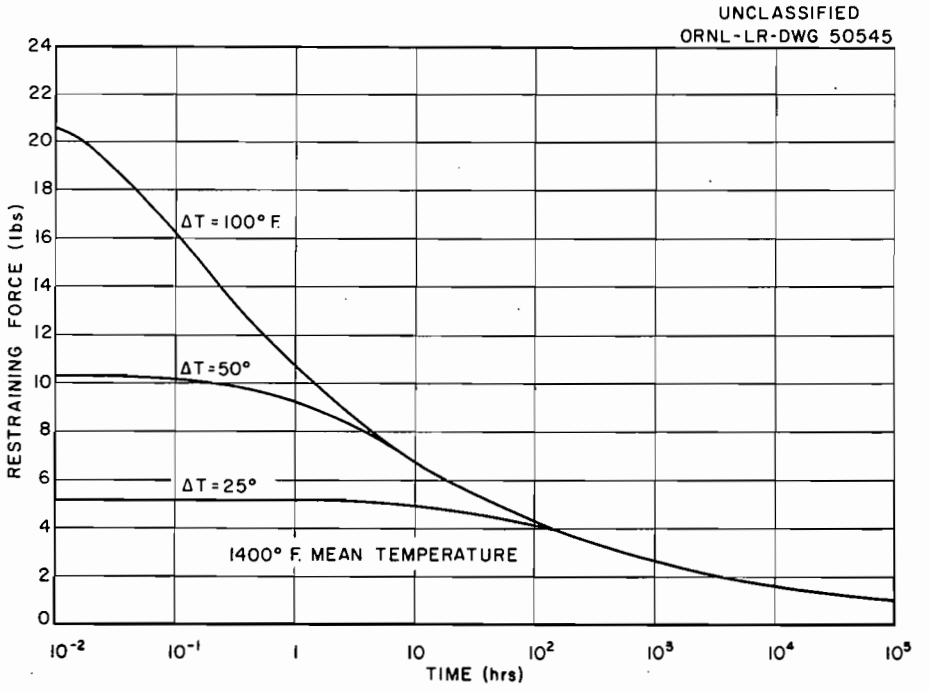

Fig. 11. Force Necessary to Restrain Midpoint of EGCR Fuel Rod as a Function of Time for a Mean Temperature of 1400°F and Diametrical Temperature Differences of 25, 50, and 100°F.

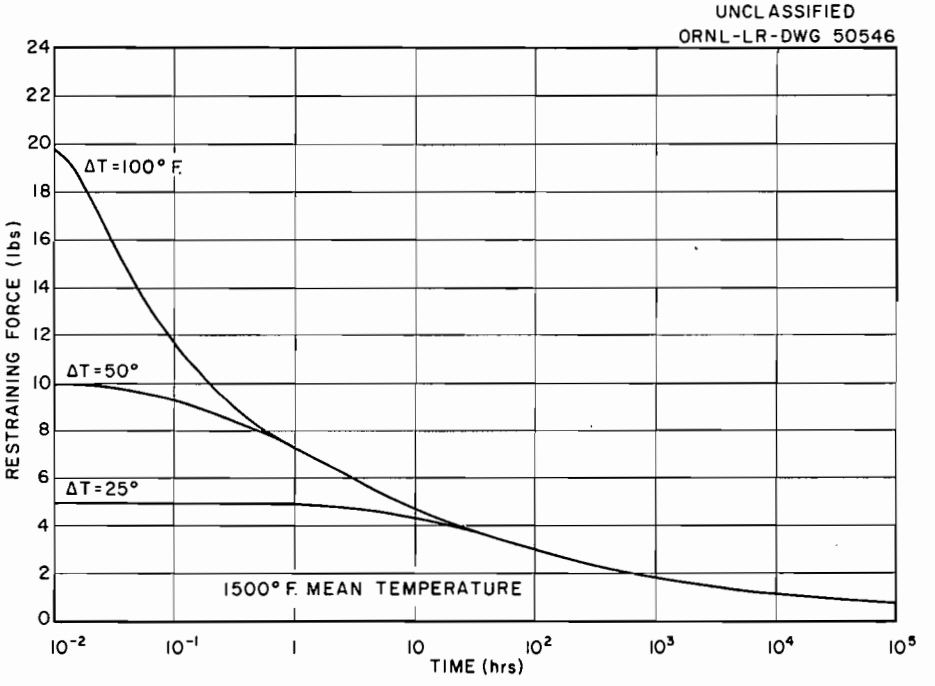

Fig. 12. Force Necessary to Restrain Midpoint of EGCR Fuel Rod as a Function of Time for a Mean Temperature of 1500°F and Diametrical Temperature Differences of 25, 50, and 100°F.

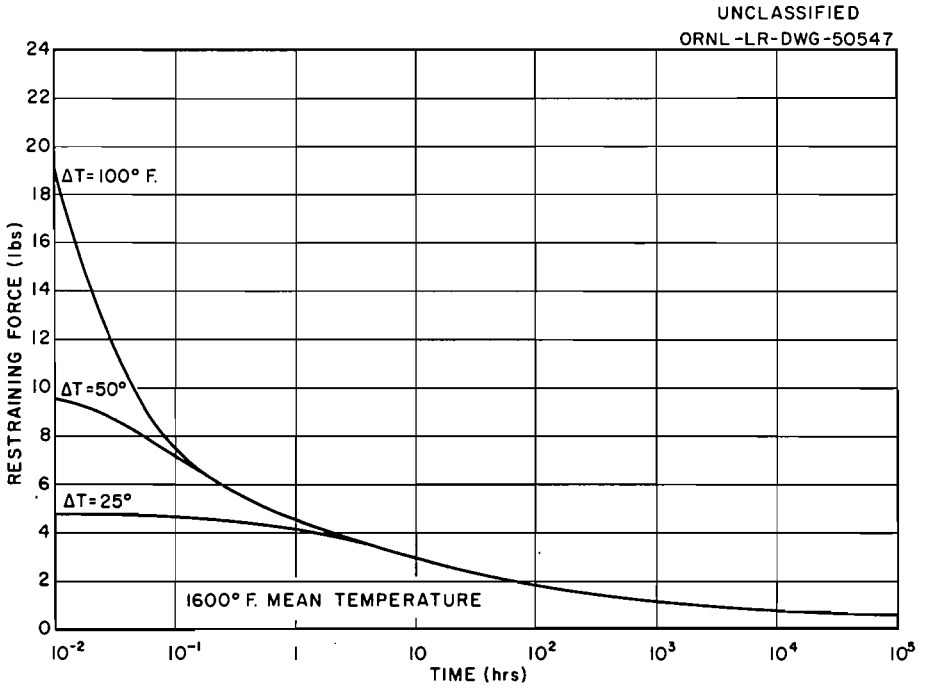

Fig. 13. Force Necessary to Restrain Midpoint of EGCR Fuel Rod as a Function of Time for a Mean Temperature of 1600°F and Diametrical Temperature Differences of 25, 50, and 100°F.

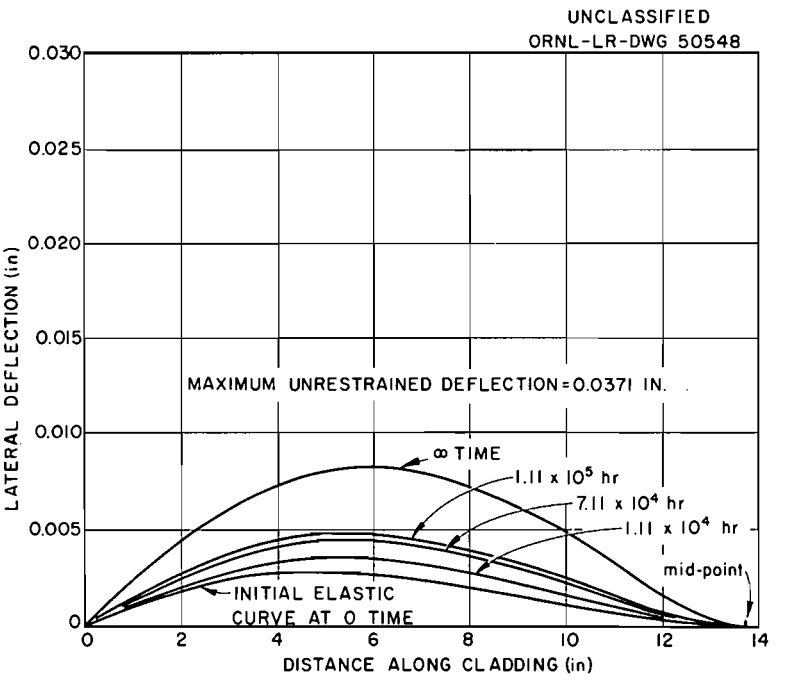

Fig. 14. Deflection of EGCR Fuel Rod Versus Distance Along Cladding for a Mean Temperature of 1200°F and a Diametrical Temperature Difference of 25°F.

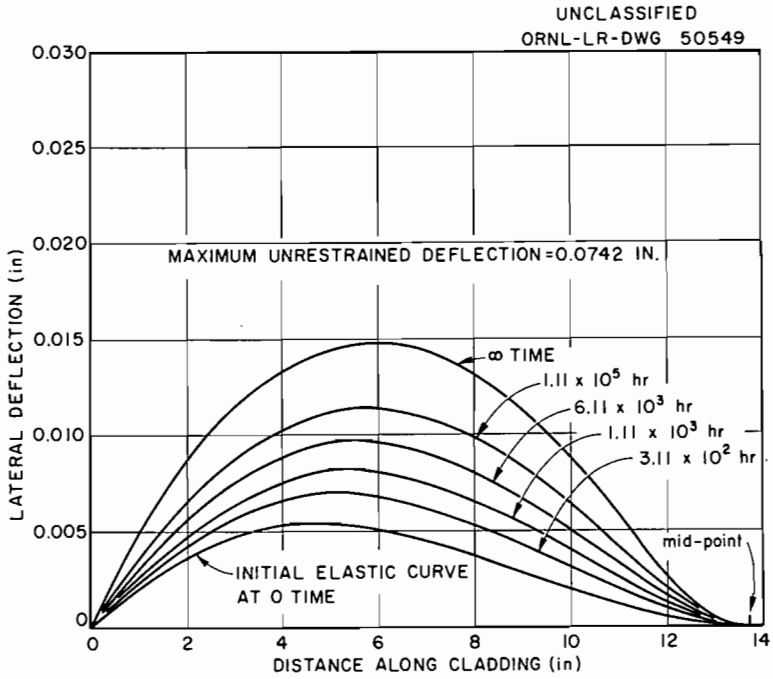

Fig. 15. Deflection of EGCR Fuel Rod Versus Distance Along Cladding for a Mean Temperature of 1200°F and a Diametrical Temperature Difference of 50°F.

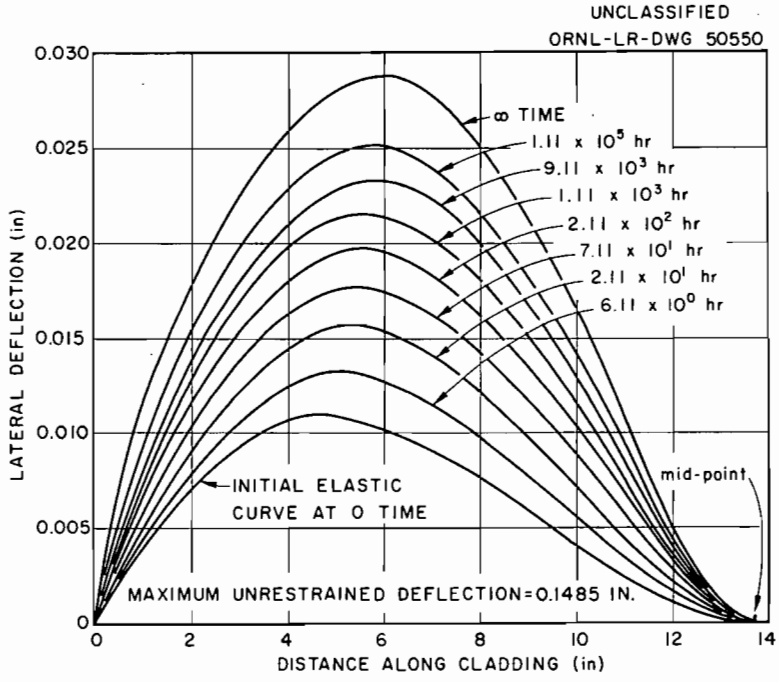

Fig. 16. Deflection of EGCR Fuel Rod Versus Distance Along Cladding for a Mean Temperature of 1200°F and a Diametrical Temperature Difference of 100°F.

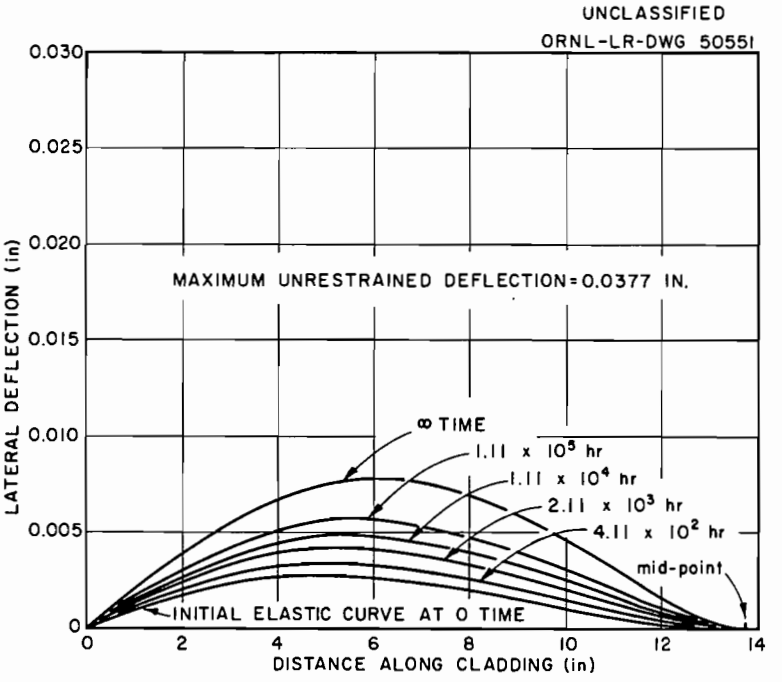

Fig. 17. Deflection of EGCR Fuel Rod Versus Distance Along Cladding for a Mean Temperature of 1300°F and a Diametrical Temperature Difference of 25°F.

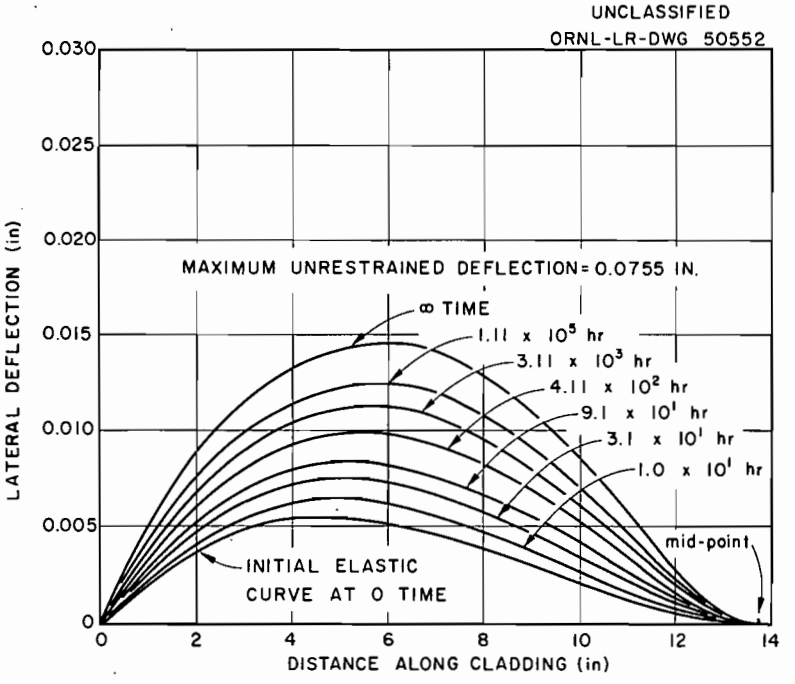

Fig. 18. Deflection of EGCR Fuel Rod Versus Distance Along Cladding for a Mean Temperature of 1300°F and a Diametrical Temperature Difference of 50°F.

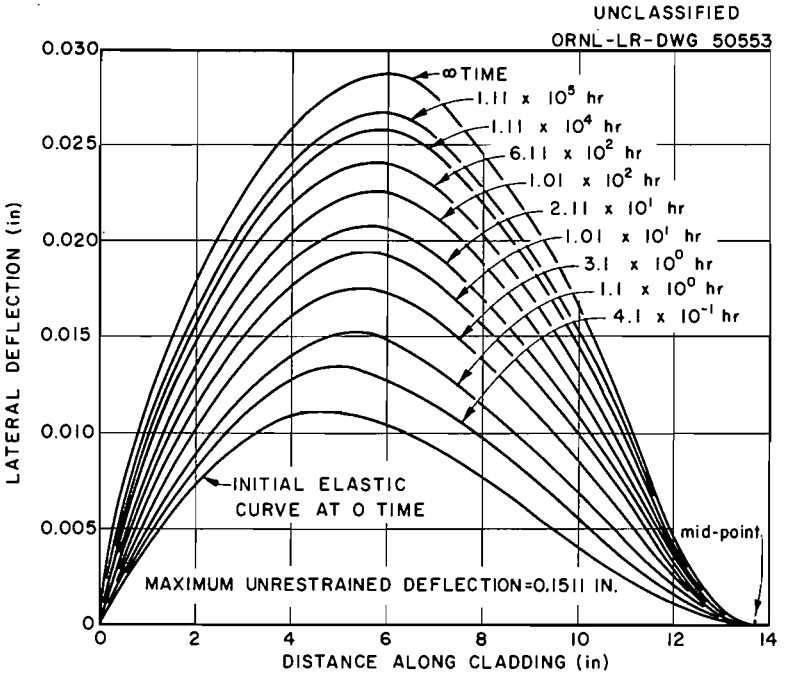

Fig. 19. Deflection of EGCR Fuel Rod Versus Distance Along Cladding for a Mean Temperature of 1300°F and a Diametrical Temperature Difference of 100°F.

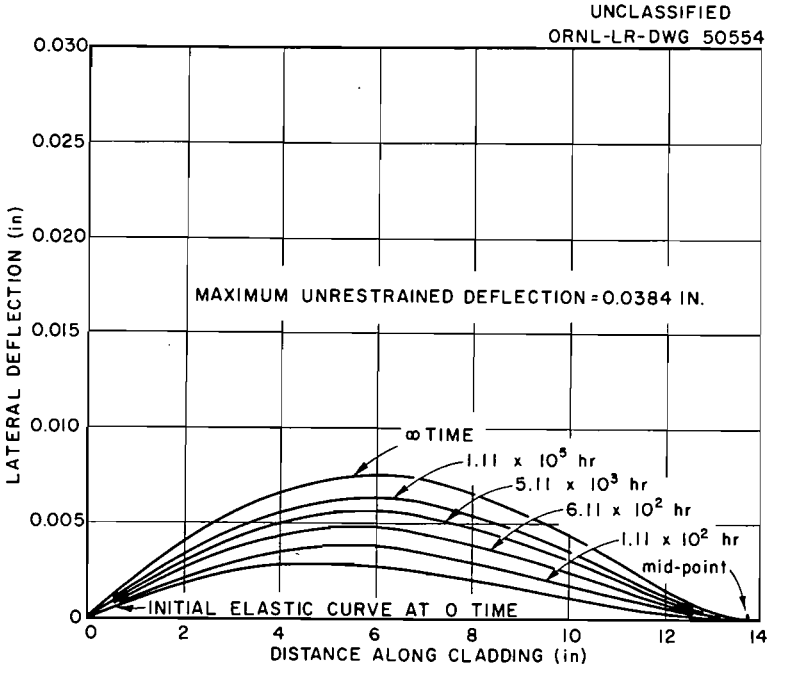

Fig. 20. Deflection of EGCR Fuel Rod Versus Distance Along Cladding for a Mean Temperature of 1400°F and a Diametrical Temperature Difference of 25°F.

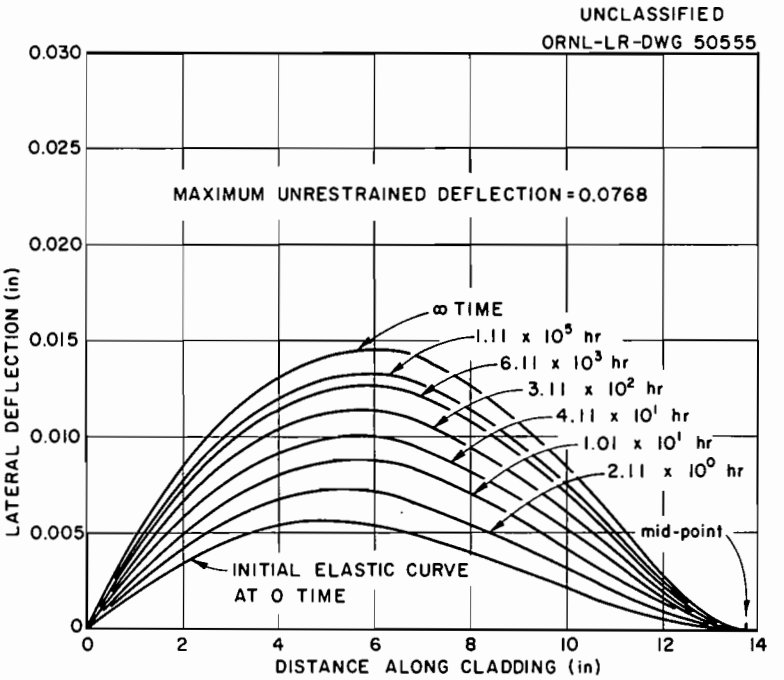

Fig. 21. Deflection of EGCR Fuel Rod Versus Distance Along Cladding for a Mean Temperature of 1400°F and a Diametrical Temperature Difference of 50°F.

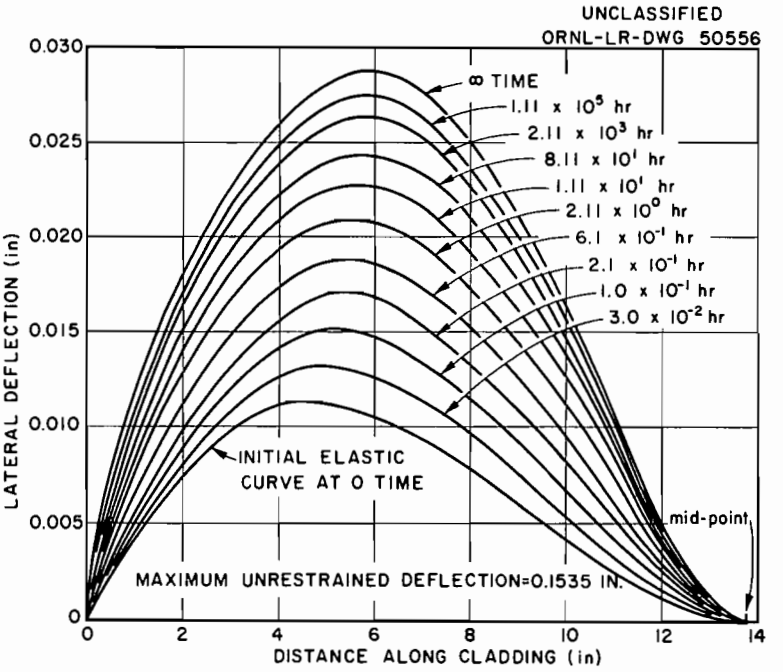

Fig. 22. Deflection of EGCR Fuel Rod Versus Distance Along Cladding for a Mean Temperature of 1400°F and a Diametrical Temperature Difference of 100°F.

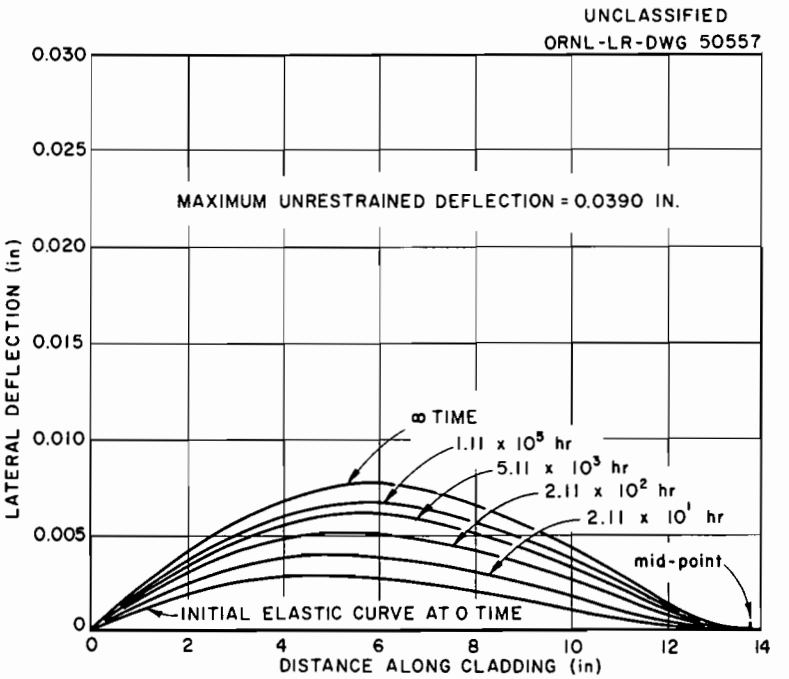

Fig. 23. Deflection of EGCR Fuel Rod Versus Distance Along Cladding for a Mean Temperature of 1500°F and a Diametrical Temperature Difference of 25°F.

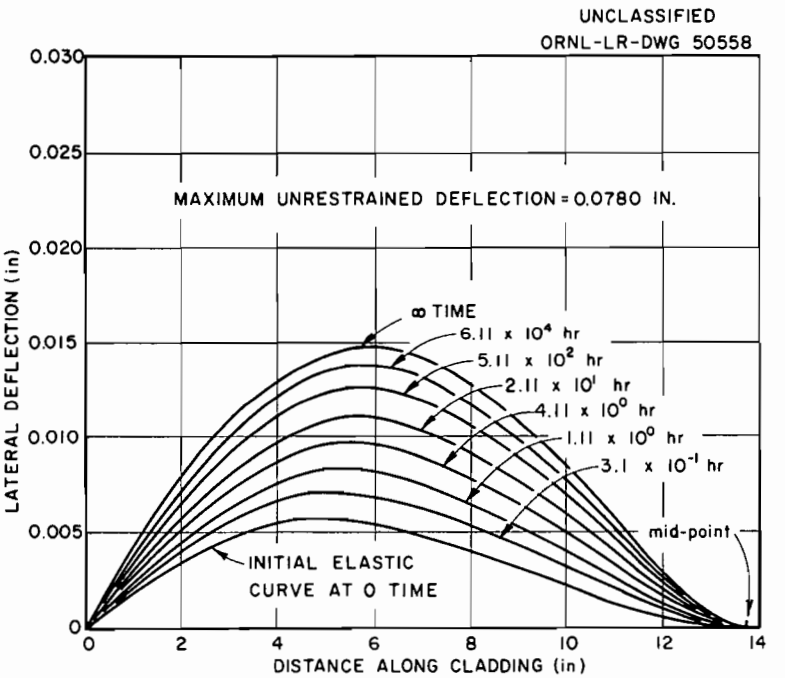

Fig. 24. Deflection of EGCR Fuel Rod Versus Distance Along Cladding for a Mean Temperature of 1500°F and a Diametrical Temperature Difference of 50°F.

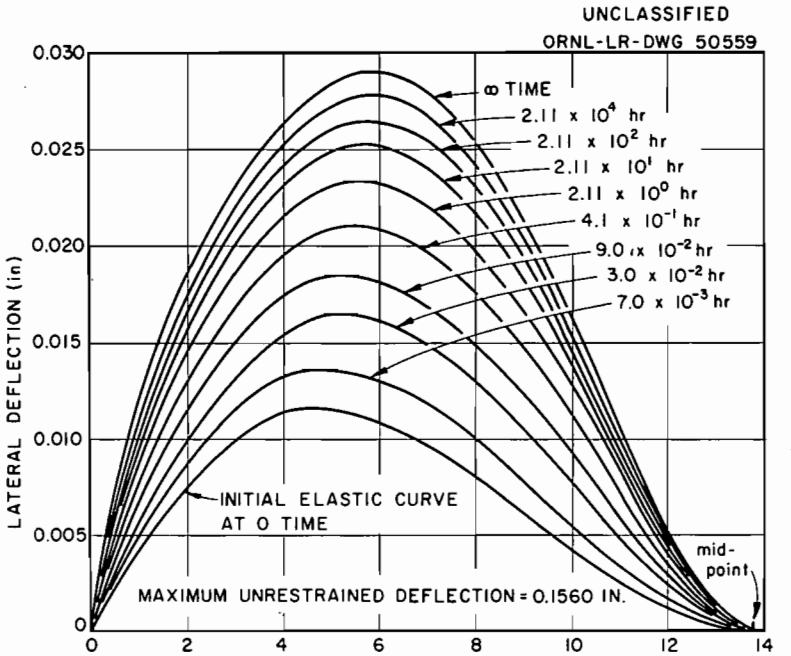

Fig. 25. Deflection of EGCR Fuel Rod Versus Distance Along Cladding for a Mean Temperature of 1500°F and a Diametrical Temperature Difference of 100°F.

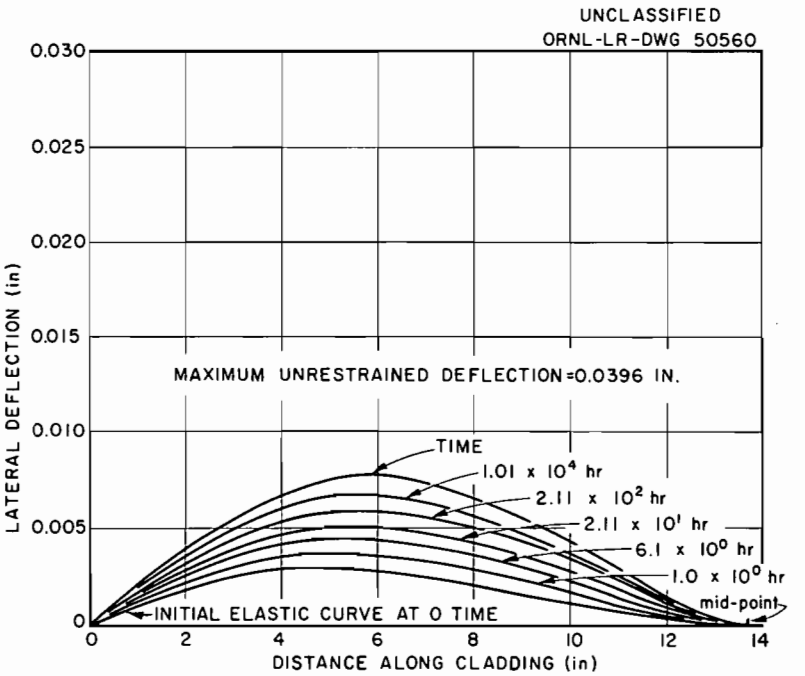

Fig. 26. Deflection of EGCR Fuel Rod Versus Distance Along Cladding for a Mean Temperature of 1600°F and a Diametrical Temperature Difference of 25°F.

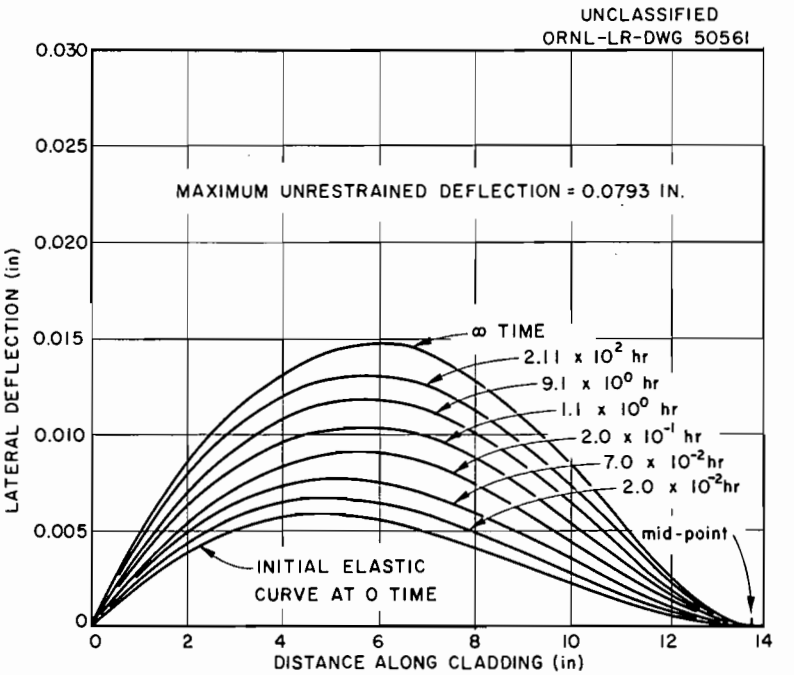

Fig. 27. Deflection of EGCR Fuel Rod Versus Distance Along Cladding for a Mean Temperature of 1600°F and a Diametrical Temperature Difference of 50°F.

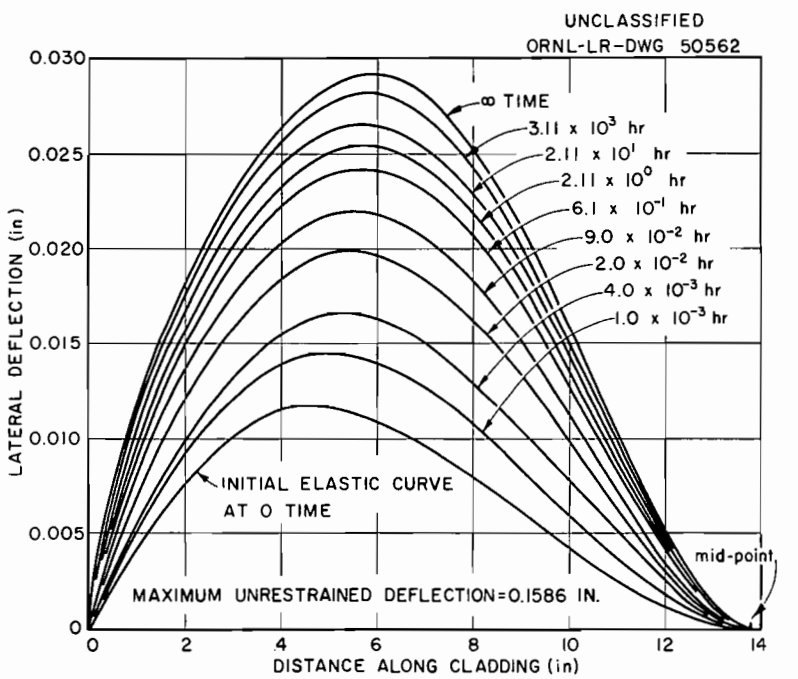

Fig. 28. Deflection of EGCR Fuel Rod Versus Distance Along Cladding for a Mean Temperature of 1600°F and a Diametrical Temperature Difference of 100°F.

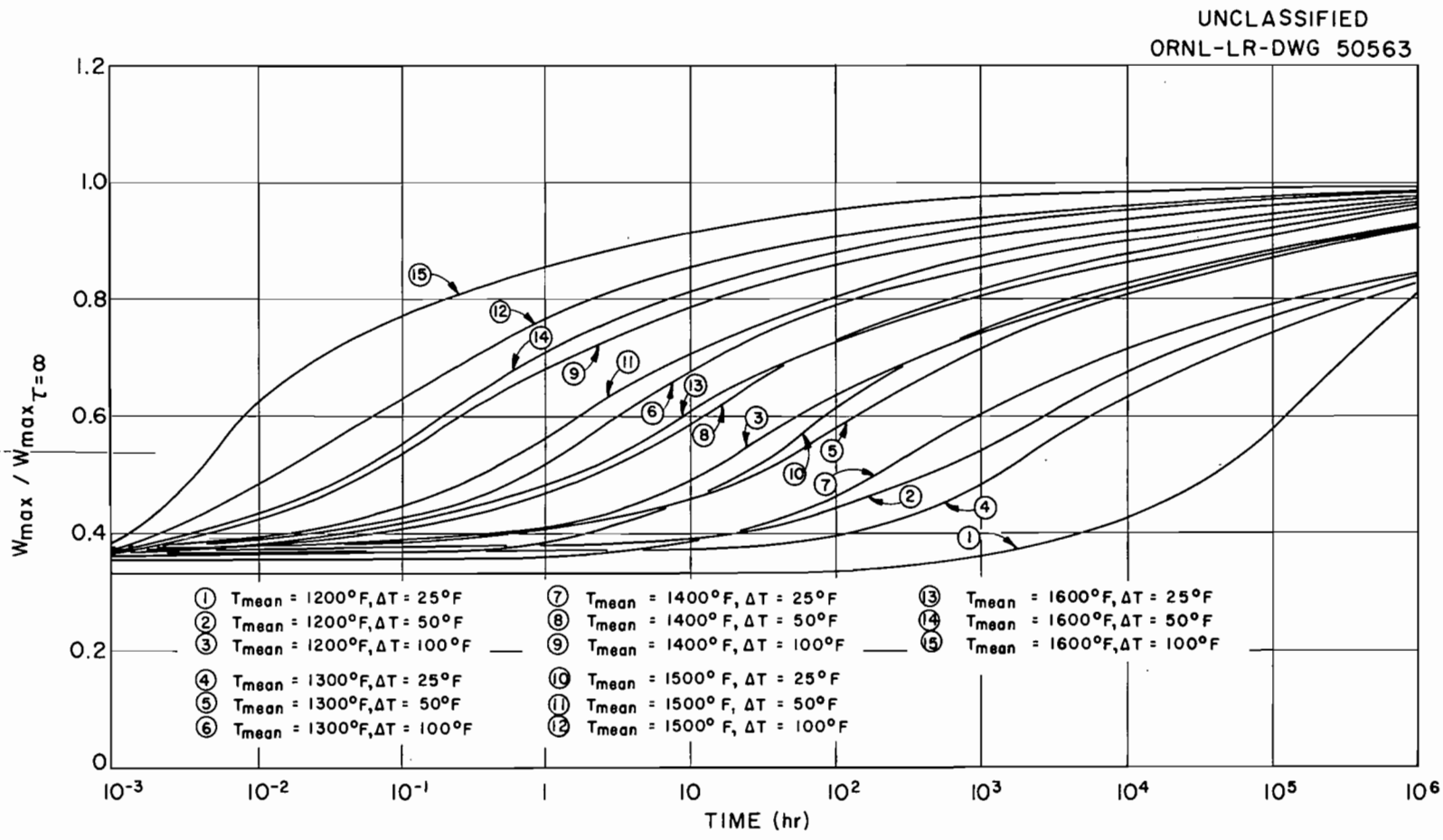

Fig. 29. Ratio of Maximum Deflection at Time τ to Maximum Deflection at $\tau = \infty$ for EGCR Fuel Rod at the Mean Temperatures and Diametrical Temperature Differences Indicated.

UNCLASSIFIED
ORNL-LR-DWG 50564

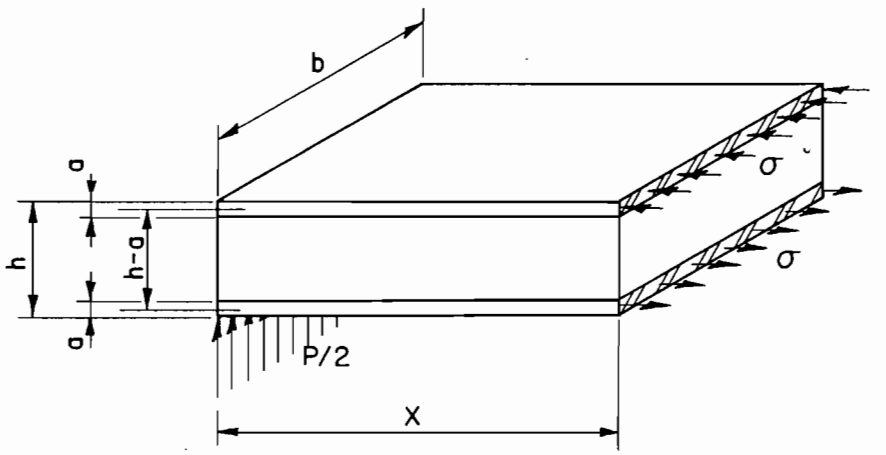

FIG. A1

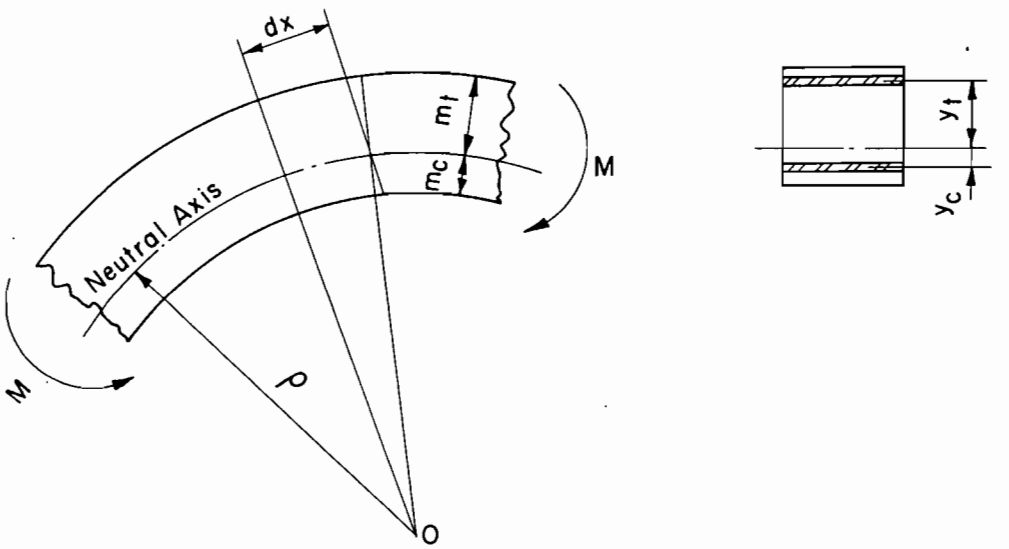

FIG. B1

UNCLASSIFIED
ORNL-LR-DWG 50565

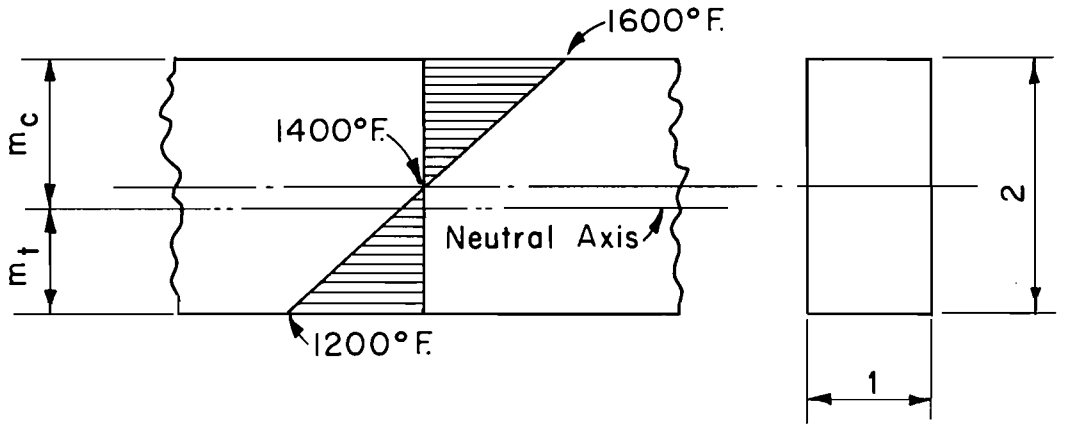

FIG. B2

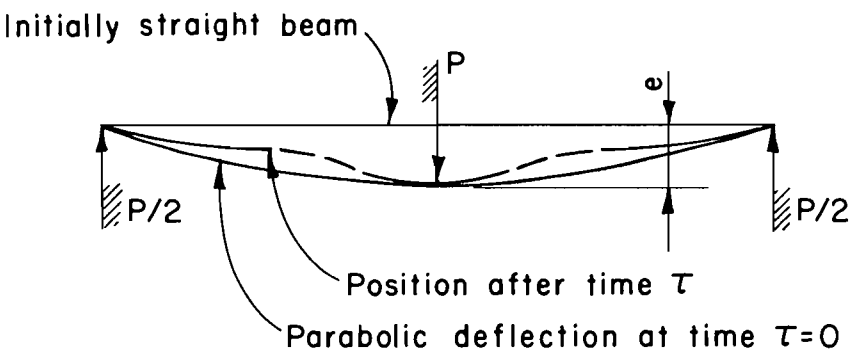

FIG. C1

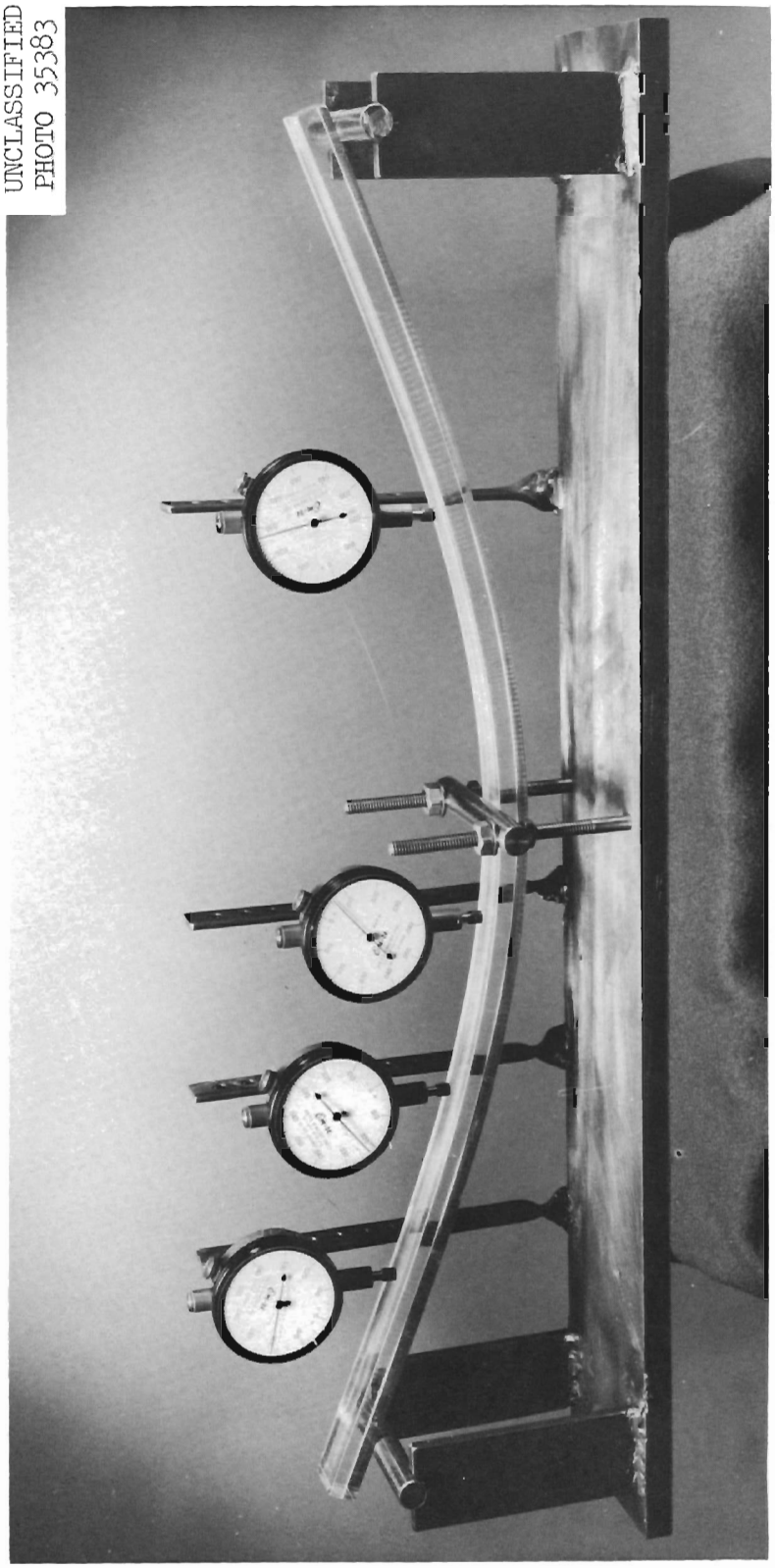

Fig. C2. Plexiglas Beam Test.

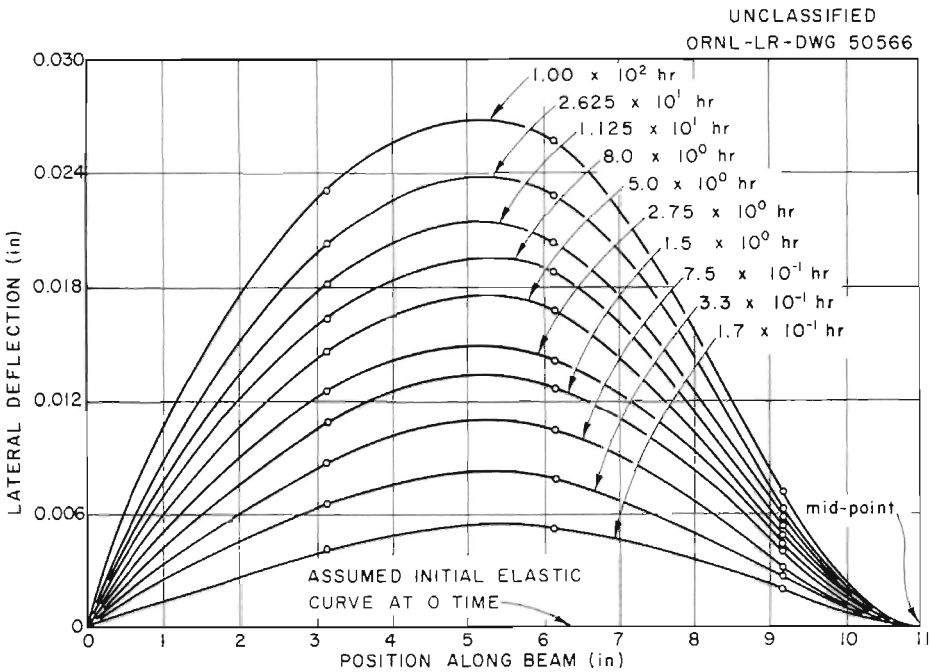

Fig. C3. Deflection Versus Distance Along Plexiglas Beam With a Maximum Initial Deflection of Three Inches.

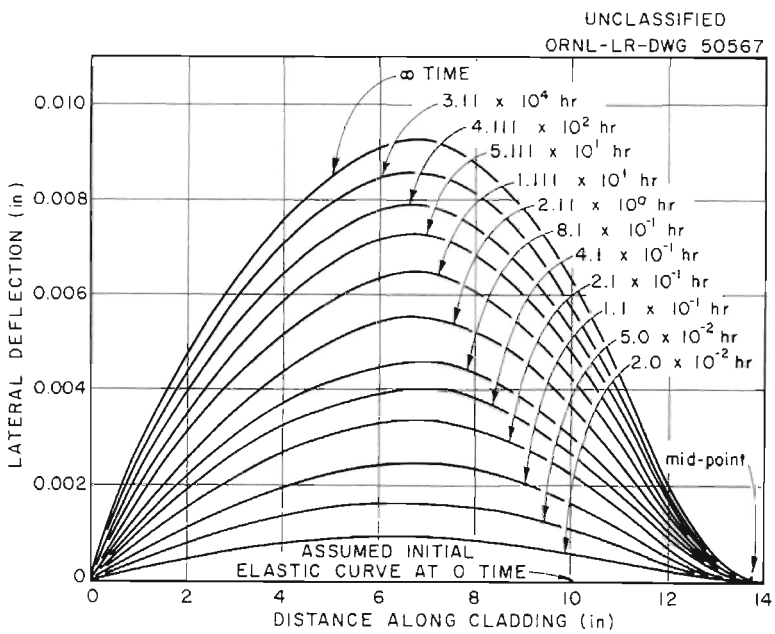

Fig. C4. Deflection of EGCR Fuel Rod Versus Distance Along Cladding for a Mean Temperature of 1600°F, a Diametrical Temperature Difference of 50°F, and an Assumed Straight Line Initial Elastic Curve.

Internal Distribution

1. S. E. Beall
2. J. M. Corum
3. B. L. Greenstreet
4. R. N. Lyon
5. J. G. Merkle
6. I. Spiewak
7. J. R. Weir
8. G. T. Yahr

9-10. Central Research Library (CRL)
11-12. Document Reference Section (DRS)
13-15. Laboratory Records (LRD)
16. Laboratory Records (LRD-RC)
17-31. Division of Technical Information Extension (DTIE)
32. Research and Development Division
33. Reactor Division (ORO)
34. ORNL Patent Office

External Distribution

35. H. Lawrence Snider, Lockheed Aircraft Corporation
36. W. E. Crowe, Los Alamos Scientific Laboratory
37. E. O. Bergman, National Engineering Science Co.
38. B. F. Langer, Bettis Plant, Westinghouse
39. A. I. Chalfant, Pratt and Whitney Aircraft